Published by

British Journal of Contemporary Research

BEXFORD PUBLISHING

Extended Stochastic Logistic Growth Model with Population Dynamics: Development and Simulation

Original Research Article | Volume 1 | Issue 6 | 2026 | Article Number: 076

Accepted: 03 November 2026 | Published: 10 November 2026 | ISSN: 2979-8582 (Online)

Crossref : **https://doi.org/10.67693/BJCR-WBK4QHKS**

Ikegwu, Emmanuel M.[1], Nkemnole, E. Bridget[2], Arowolo, O. Taofik[3]

[1]Department of Statistics, Faculty of Physical and Earth Science, University of Lagos, Akoka, Nigeria; Department of Statistics, School of Science, Yaba College of Technology, Yaba, Lagos, Nigeria,

[2]Department of Statistics, Faculty of Physical and Earth Science, University of Lagos, Akoka, Nigeria,

[3]Department of Mathematical Sciences, Faculty of Science, Lagos State University of Science and Technology, Ikorodu, Lagos, Nigeria; Department of Statistics, Faculty of Physical and Earth Science, University of Lagos, Akoka, Nigeria

IEM 0000-0002-0681-6006

Correspondence: Ikegwu, Emmanuel M., emmanuel.ikegwu@yabatech.edu.ng

Abstract

Population growth in developing economies presents complex challenges, requiring robust models to inform sustainable policy interventions. This literature review examines the classical Stochastic Logistic Growth Models (SLGMs), and proposes a Population Dynamics Extension to it as an advanced framework integrating stochasticity, carrying capacity and population dynamics to better capture real-world demographic fluctuations. Unlike classical logistic models, the Extended SLGM with population dynamics accounts for environmental stressors, economic constraints, and policy-driven population control measures, making it particularly relevant for developing nations grappling with rapid urbanisation and resource scarcity. This review synthesises key studies applying the SLGM and creates scenarios of extensions with births, deaths and migration rates, and resource constraints, highlighting its superiority over deterministic approaches in predicting growth trajectories under uncertainty and over the classical SLGM. Special emphasis is placed on how the model informs policies balancing economic development with demographic stability. Critically, we identify gaps in current research, such as the need for localised parameter calibration and interdisciplinary integration with socio-economic data. By evaluating the extended SLGM with Population Dynamics, its theoretical and empirical contributions will be explored, with its potential as a tool for policymakers seeking evidence-based strategies to manage population growth in developing economies while fostering equitable development.

Keywords: Demographic Modelling, Developing Economies, Growth Control, Population Dynamics, Stochastic Logistic Growth, Sustainable Development

© 2026 The Authors. Published by Bexford Publishing Ltd

Introduction

Classical population growth models started with the Malthus model proposed by Thomas Malthus in the 18th century, which argued that under stable environmental conditions, populations grow or decline exponentially. However, this model captured the explosive potential of unchecked growth but lacked realism when resources became limited (Malthus, 1898). Modifications of the model were introduced in the 19th century by mathematicians who introduced mortality–focused refinements by proposing logistic growth models (Gompertz, 1825; Verhulst, 1838). Verhulst's equation was given as:

$$dP = (rP - \alpha P)dt \quad (1)$$

Where r is the intrinsic growth rate, P is the population size, and the carrying capacity of the equilibrium K is $\frac{r}{\alpha}$. The logistic equation was later popularised by Pearl & Reed (1920), who promoted the model in ecology and demography as:

$$dP = rP\left(1 - \frac{P}{K}\right)dt \quad (2)$$

With an explicit solution that forms a sigmoidal or S-shaped curve, it is generally known as a deterministic model. This model sits at the crossroads of demography, ecology, mathematical biology, epidemiology and finance, offering a simple but powerful description of growth moderated by resource constraints (Caswell, 2019; Kawano et al., 2020; Zinihi et al., 2025).

With the unpredictability of nature, this deterministic model fails to account for random influences, namely, environmental variability, demographic chance, and sudden shocks. This gave rise to the stochastic logistic growth model by introducing randomness into the growth rate via a noise term often modelled as white noise (a Wiener process) in a stochastic differential equation (SDE). The stochastic logistic growth model is given as:

$$dP_t = rP_t\left(1 - \frac{P_t}{K}\right)dt + \sigma P_t dW_t \quad (3)$$

Where σ captures the intensity of environmental stochasticity, and W_t is the Wiener process (Ferreira, 2014; DiLeonardo, 2018). These SDEs are simulated using methods like the Euler-Maruyama method to generate sample paths. Studies show that such sample paths exhibit fluctuations around the deterministic trajectory, and depending on the noise intensity, the population may even go extinct, even when mean conditions would predict persistence (Ferreira, 2014; Mendez et al, 2015; Bayram et al., 2018; Ikegwu & Nkemnole, 2025; Zinihi et al., 2025). Hence, stochastic logistic models bring realism by accounting for randomness and allow for quantifying important aspects like risk extension, variance around equilibrium and time to threshold crossing.

Population dynamics is a broad field concerning how populations change over time under the influence of births, deaths, migration, competition and resource availability. Historically, it stretches more than two centuries, beginning with Malthusian exponential growth and evolving through the logistic model and beyond (Guo, 2014; Stutz, 2014; Taagepera & Nemcok, 2023; Sojecka & Drozd-Rzoska, 2024; Akber et al., 2025). Some of the key developments of population dynamics modelling include the structured population models like the Euler-Lotka equation, which tracks age-specific survival and fecundity over time. This integral (or discrete sum) equation helps to determine the population's growth rate through the growth rates via species' life history traits (Caswell et al., 2018; Caswell, 2019; Kozlov et al., 2021; Hernandez-Suarez, 2023). Another is the predator-prey models (Lotka-Volterra) and their generalisations, like the Kolmogorov population model (1936), include multiple species interactions, stability analysis,

© 2026 The Authors. Published by Bexford Publishing Ltd

oscillations and complex dynamics (Sigmund, 2007; Alebraheem, 2021; Tarasov, 2021; Ogethakpo & Ojobor, 2021; Wang & Niu, 2025). Population dynamics aims to describe and predict patterns like logistic-type saturation, cycles, boom-bust and extinction under both deterministic and stochastic influences. Hence, it provides frameworks from single-species logistic dynamics to multi-species interactions and structured populations capturing real ecological complexity.

Merging stochastic logistic modelling with a population dynamics framework brings together realism and biological structure. Deterministic population dynamics models can be extended to stochastic differential equations or Markov chain frameworks that accommodate randomness (McKane & Newman, 2004; Hu et al., 2018; Rihan & Alsakaji, 2020; Zhao & Niu, 2024). For instance, the stochastic logistic growth model is extended beyond the single-population logistic form to Lotka-Volterra dynamics with noise. Two classes of stochastic logistic model have been outlined, which are environmental randomness with noise directly added to growth rate, as shown in the SDE and demographic randomness building from individual-level birth-death rates via diffusion approximations leading to SDEs whose drift and diffusion reflect population events (Ferreira, 2014; Di Crescenzo & Paraggio, 2019; Al Husain & Al-Eideh, 2022). Simulation using these models reveals richer behaviours, including stochastic extinction, fluctuating equilibria and path-dependent outcomes.

Also, models where individual birth and death events are stochastic at the micro-level can, under large population limits, give rise to stochastic logistic dynamics at the macro-level. Significant strides were made by deriving logistic-type SDEs from underlying microscopic rules, quantifying precisely extinction probabilities and times to extinction using advanced mathematical tools like spectral theory and Wentzel, Kramers and Brillouin (WKB) or Liouville-Green approximations (Padilla, 2012; Mendez et al., 2015; Berman, 2017; Czuppon & Traulsen, 2021; Marrec et al., 2023). This approach grounds the stochastic logistic model in mechanistic fundamentals and links macroscopic parameters (like r, K) to microscopic birth-death parameters, critical for ecological interpretation and parameter estimation (Grilli, 2020; Simpson et al., 2022). These extensions put together enrich the classical model by aligning it with population structure, random fluctuations and realistic ecological interactions.

Beyond formulating stochastic models, the field has developed deep theoretical frameworks to understand their dynamics, long-term behaviour and biological implications. Deterministic models, even when they predict stable carrying capacity, stochastically introduce extinction risk. Analytically, methods like WKB approximations and spectral approaches allow the estimation of mean time to extinction, invasion probabilities and persistence thresholds (Mubayi et al., 2019; Badali & Zilman, 2020; Feng et al., 2022; Pelagalli et al., 2025). Also, researchers derive probability distributions of the population size over time, examine variance growth and describe confidence intervals around the mean trajectory. Stochastic Malthusian and logistic models allow closed-form derivation of standard deviation dynamics, revealing how uncertainty spreads over time (Heydari et al., 2014; Bradshaw & Herrando-Perez, 2023; Baltazer-Larios et al., 2025).

Environmental stochasticity measures random fluctuations in the environment that affect all individuals modelled as noise in birth-death rate or growth terms. Also, Demographic stochasticity measures randomness due to discrete birth/death events at the individual level, especially in small populations (Browning et al., 2020; Tesfay et al., 2021; Yu & Ma, 2023). Each of these has different mathematical implications, as environmental noise often leads to multiplicative SDEs while demographic noise may require jump-diffusion or birth-death process models. (Pearl & Reed, 1920)

Also, theoretical work often explores how discrete, random birth-death processes converge to continuous SDEs under diffusion approximations, while theories address the stochastic stability of equilibria, whether

© 2026 The Authors. Published by Bexford Publishing Ltd

the population fluctuate around a deterministic equilibrium, or noise drives it to extinction or expansion Di Crescenzo et al., 2021; Ignatieva et al., 2020; Chen et al., 2023). This examines the stationary distribution of the SDE and its properties. Lastly, linking theoretical models to data requires estimating parameters like r, K and noise intensity σ. Microscopic modelling provides a bridge by interpreting these as functions of the underlying birth/death rate, facilitating more grounded inference (Veron et al., 2025; Shoemaker et al., 2025).

Methodology

Usman (2025) proposed an enhanced Logistic growth model that incorporated population dynamics like birth, death, net migration rates and economic limitations into the Verhulst Logistic growth model to derive:

$$\frac{dP}{dt} = \rho P\left(1 - \frac{P}{K}\right) + bP - dP + \mu P + L \quad (5)$$

Where

$P(t)$ is the population at time t; ρ is the intrinsic growth rate; b represents the birth rate, d represents the death rate, μ represents net migration, and L represents the resource limitations, respectively.

It showed that population growth is not only affected by the intrinsic rate of growth and the carrying capacity, but also the rate of births, deaths and net migration in the population, coupled with the limitations imposed by the economy. The model thus implies that where these dynamics are zero, i.e., $bP = 0$, $dP = 0$, $\mu P = 0$ and $L = 0$, the model reverts to the classical logistic model. This has been the latest extension of the logistic growth model and is deterministic altogether. Usman (2025) estimated the parameters of the enhanced logistic growth model using the Runge-Kutta-Felberg 4-5 methods.

The stochastic logistic growth model extended with population dynamics (PD-SLGM), obtained by extending Usman's model with a stochastic component and presented as the stochastic differential equation (SDE), is given below.

$$dP(t) = rP(t)\left(1 - \frac{P(t)}{K}\right)dt + bP(t)dt - aP(t)dt + mP(t)dt + Ldt + fP(t)dW(t) \quad (6)$$

Where $P(t)$ is the population at time t; r is the intrinsic growth rate; b represents the birth rate, d represents the death rate, m represents net migration, L is the resource limitations, f is the noise intensity, and W_t is the standard Wiener process or Brownian motion, respectively

$$dP(t) = \left[rP(t)\left(1 - \frac{P(t)}{K}\right) bP(t) - aP(t) + mP(t) + L\right]dt + fP(t)dW(t) \quad (7)$$

$$= \left[rP(t)\left(1 - \frac{P(t)}{K}\right) + (b - a + m)P(t) + L\right]dt + fP(t)dW(t) \quad (8)$$

Let

$$\lambda = (b - a + m) \quad (9)$$

Substituting equation (9) into equation (8)

$$= \left[rP(t)\left(1 - \frac{P(t)}{K}\right) + \lambda P(t) + L\right]dt + fP(t)dW(t) \quad (10)$$

Equation (10) is the Stochastic Logistic Growth Model with Population Dynamics (PD-SLGM) proposed in this study.

This specification allows the model to capture not just limiting population growth but also the influence of demographic forces and random environmental fluctuations, aligning with real-world settings in

© 2026 The Authors. Published by Bexford Publishing Ltd

developing economies (Gardner, 2009; Allen, 2015).

Equation (10) is a stochastic differential equation (SDE) which is analysable within the Ito framework, where the drift term represents the deterministic growth force and is given in equation (11), and the diffusion term captures stochastic noise and is given in equation (12).

The drift term $\mu(P)$ as:

$$\mu(P) = rP\left(1 - \frac{rP}{K}\right) + \lambda P + L \quad (11)$$

And the diffusion term $\sigma(P)$ as:

$$\sigma(P) = fP;\ \sigma^2(P) = f^2P^2 \quad (12)$$

The structure of equations (11) and (12) ensures positivity of the process as the noise scales with population size and aligns with biological realism, as larger populations experience proportionally greater stochastic variability (Kloeden & Platen, 1999; Allen, 2015).

In an increasingly volatile world marked by demographic transitions, security-induced displacements, climate-driven displacements, resource constraints and socioeconomic inequality, understanding and modelling population growth dynamics requires models that go far beyond linear or deterministic trajectories. Classical deterministic logistic models or their enhancements, and the classical stochastic logistic models or their extensions so far fall short of explaining real-world fluctuations in population influenced by complex forces like birth surges, migration shocks, mortality shifts and environmental limits. Though traditional models are elegant, they are detached from the chaotic fabric of modern population dynamics. To bridge this gap, this study also proposed a new demographic modelling approach, the extended stochastic logistic growth model with population dynamics (PD-SLGM). Unlike conventional models, the PD-SLGM integrates demographic components, birth rate, death rate, migration rate and environmental resources constraints, allowing population to evolve under demographic, structural and random forces, making it responsive to economic policy shifts, migration dynamics, fertility transitions and public health investments (Prettnet & Bloom, 2020; UN DESA, 2024).

One of the greatest strengths of the PD-SLGM is its interpretability, as each term in the model reflects a real-world process, which makes it a policy-sensitive model. For instance, by tuning L and λ, planners can simulate how increasing access to resources or reducing maternal mortality influences long-term population sustainability. The stochastic formulation offers confidence bands and probabilistic forecasts, which are critical in development planning, disaster response and urban management (World Bank, 2025).

Hence, in a world where population questions are tied to public health, urban planning, climate justice and migration ethics, the PD-SLGM offers a rigorous, flexible and interpretable framework. It serves both academic demographers and policy planners, offering not just forecasts but a deep understanding of the uncertainty that surrounds them.

Estimating the Model Parameters Using the Euler Pseudo Log-Likelihood Methods

The stochastic logistic growth model extended with population dynamics given in equation (10) has parameters $\theta = (r, K, \lambda, L, f)$. Using the Euler pseudo-likelihood to closed -form results in an optimisation routine, to obtain approximate Fisher-Information formulae for standard errors, and alternative moment/ regression estimators.

Setting up Small (Δ_i) Approximation

© 2026 The Authors. Published by Bexford Publishing Ltd

Assume observations P_{i_o}, P_{i_1}, ..., P_{i_n}, taken at equal intervals $\Delta t = t_{i+1} = t_i$, and assume Δt is small enough that the Euler-Maruyama approximation is reasonable (Kloeden & Platen, 1999). Given the drift in equation (11) and the diffusion in equation (12), for small Δt, the transition $P_{i+1}|P_i$ is approximated as Gaussian:

$$P_{i+1}|P_i \approx N\left(P_i + \mu\left(P_i; \theta\right)\Delta t,\ \sigma^2\left(P_i; \theta\right)\Delta t\right) \tag{13}$$

Introducing the increment $\Delta_i = P_{i+1} - P_i$ and the short-hand variance

$$V_i(\theta) = \sigma^2\left(P_i; \theta\right)\Delta t = f^2 P_i^2 \Delta t \tag{14}$$

The Gaussian approximation underpins the Euler pseudo-likelihood (EPL) (Jalal & Alarid-Escudero, 2017; Bibby & Sorensen, 1995).

Euler Pseudo-Log-Likelihood (EPL)

The conditional density for the i[th] increment (approx.) is given as:

$$p_\theta\left(P_i\right) = \frac{1}{\sqrt{2\pi V_i(\theta)}}\exp\ exp\left\{-\frac{\left(\Delta_i - \mu\left(P_i;\theta\right)\Delta t\right)^2}{2V_i(\theta)}\right\} \tag{15}$$

The log-likelihood for the whole series (up to an additive constant) is:

$$l(\theta) = -\frac{1}{2}\sum_{i=1}^{n-1}\left[log\ V_i(\theta) + \frac{\left(\Delta_i - \mu_i \Delta t\right)^2}{V_i(\theta)}\right] \tag{16}$$

The $l(\theta)$ in equation (16) is maximised (or the negative log-likelihood is minimised),

Score (Gradient) Derivation

Let $S_i(\theta) := \Delta_i - \mu_i \Delta t$ denote the residual for interval I, for general parameter η (one coordinate of θ), differentiate $l(\theta)$ in equation (16), using the chain rule. Begin with the compact identity (after brief algebraic manipulation). For parameters that do not enter the variance $V_i(\theta)$ (that is r, K, λ, L), the second term disappears, giving a simpler score expression. Hence, differentiating $-\frac{1}{2}\left[\log log\ V_i + \frac{S_i^2}{V_i}\right]$ with respect to η and collecting like terms (using quotient and chain rules),

$$\frac{\partial l}{\partial \eta} = \sum_{i=1}^{n-1}\left[\frac{S_i(\theta)\Delta t}{V_i(\theta)}\frac{\partial \mu}{\partial \eta} - \frac{1}{2}\frac{V_i(\theta) - S_i(\theta)^2}{V_i(\theta)^2}\frac{\partial V_i(\theta)}{\partial \eta}\right] \tag{17}$$

Simplification for Structural Parameters (r, K, λ, L)

For $\eta \in r,\ K,\ \lambda,\ L$, and setting $\frac{\partial V_i}{\partial \eta} = 0$

$$\frac{\partial l}{\partial \eta} = \sum_i \frac{S_i(\theta)\Delta t}{V_i(\theta)}\frac{\partial \mu}{\partial \eta} \tag{18}$$

Using $V_i = f^2 P_i^2 \Delta t$, the factor $\frac{\Delta t}{V_i}$, hence,

© 2026 The Authors. Published by Bexford Publishing Ltd

$$\frac{\partial l}{\partial \eta} = \sum_{i=1}^{n-1} \frac{S_i(\theta)}{f^2 P_i^2} \frac{\partial \mu(P_i;\theta)}{\partial \eta}, \qquad for\ \eta \in (r,\ K,\ \lambda,\ L) \tag{19}$$

This is convenient because it isolates the dependence in a simple weighting by $\frac{1}{(P_i^2)} = P_i^{-2}$

Computing the derivatives of the drift function $\mu(P;\theta)$:

$$\frac{\partial \mu}{\partial r} = P - \frac{P^2}{K} = P\left(1 - \frac{P}{K}\right) \tag{20}$$

$$\frac{\partial \mu}{\partial K} = \frac{rP^2}{K^2} \tag{21}$$

$$\frac{\partial \mu}{\partial \lambda} = P \tag{22}$$

$$\frac{\partial \mu}{\partial L} = 1 \tag{23}$$

Hence, the score components are explicit functions of the data and current parameter guesses.

Score for the Diffusion Intensity f

Because $V_i = f^2 P_i^2 \Delta t$ depends on f, but μ does not; the first term disappears, leaving only the diffusion term, which reduces to

$$\frac{\partial l}{\partial f} = -\frac{1}{2} \sum_i \frac{V_i - S_i^2}{V_i^2} \cdot \frac{\partial V}{\partial f} = -\sum_i \frac{V_i - S_i^2}{V_i^2} \cdot f P_i^2 \Delta t \tag{24}$$

Substituting $V_i = f^2 P_i^2 \Delta t$ and simplify (using algebraic cancellations), after simplifications, the score reduces to:

$$\frac{\partial l}{\partial f} = -\frac{n}{f} + \sum_{i=1}^{n-1} \frac{S_i(\theta)^2}{f^3 P_i^2 \Delta t} \tag{25}$$

Setting $\frac{\partial l}{\partial f} = 0$ and solving for yields a closed-form estimator (conditional on other parameters):

$$\sum_{i=1}^{n-1} \frac{S_i^2}{P_i^2 \Delta t} = nf^2 \Rightarrow f^2 = \frac{1}{n} \sum_{i=1}^{n-1} \frac{(\Delta t - \mu_i \Delta t)^2}{P_i^2 \Delta t} \tag{26}$$

This shows that, for fixed drift parameters, the diffusion intensity f has an explicit moment-type estimator (the square root of an average scaled residual variance). Practically, the drift parameters can be estimated numerically and then plugged in to obtain f, or all the parameters can be jointly optimised numerically.

Approximate Observed Information and Standard Errors

For inferences, the observed information (negative Hessian) is used, evaluated at the maximum likelihood estimator MLE. $\hat{\theta}$. For structural parameters (where V_i does not depend on them), the Hessian elements have the approximate form:

$$\frac{\partial^2 l}{\partial \eta_j \partial \eta_l} \approx \sum_{j=1}^{n-1} \frac{(\partial \eta_j;\mu_i)(\partial \eta_k;\mu_i)\Delta t^2)}{V_i(\theta)} + \left(term\ involving\ S_j \rightarrow zero\ at\ MLE\right) \tag{27}$$

Neglecting the S_j term (standard large sample approximation) gives the Fisher-Information approximation

© 2026 The Authors. Published by Bexford Publishing Ltd

$$I_{jk}\left(\hat{\theta}\right) \approx \sum_i \frac{\left(\partial\eta_j;\mu_i\right)\left(\partial\eta_k;\mu_i\right)\Delta t^2)}{V_i(\theta)} \tag{28}$$

Recalling that $V_i = f^2 P_i^2 \Delta t$, the factor $\frac{\Delta t^2}{V_i} = \Delta t/(f^2 P_i^2$. Thus,

$$I_{jk}\left(\hat{\theta}\right) \approx \sum_i \frac{\left(\partial\eta_j;\mu((P_i;\hat{\theta})\right)\left(\partial\eta_k;\mu(P_i;\hat{\theta})\right)\Delta t}{f^2 P_i^2} \tag{29}$$

The approximate variance-covariance of θ is $I(\theta)^{-1}$.For the diffusion f, it can be derived analytically (plugging the score form and substituting expectations at the MLE), the usual result (analogous to the normal error model) giving approximate variance is:

$$Var\left(\hat{f}\right) = \frac{f^2}{2n}, \quad so \quad SE\left(\hat{f}\right) \approx \frac{f}{\sqrt{2n}} \tag{30}$$

This is followed by approximating $S_i^2 = \approx V_i$, under the model.

Using the Milstein Pseudo Log-Likelihood Methods

The Milstein scheme, a nontrivial numerical scheme for stochastic differential equations, achieves a strong order of convergence higher than that of the Euler-Maruyama scheme (Ali et al., 2024; Huang, 2011). The Milstein - based Gaussian quasi log-likelihood (GQMLE) of the extended stochastic logistic growth model with population dynamics starts with the discretisation.

For observation times $0 = t_0 < t_1 < \cdots < t_n$with $\Delta_i = t_i - t_{i-1}$ and $P_i := P_{t_i}$, the Milstein step for a 1-D Ito SDE with multiplicative noise is (set $\Delta W_i = \sqrt{\Delta_i}\,, Z_i, \quad Z_i \sim N(0,\ 1)$)

$$P_i \approx P_{1-1} + \mu\left(P_{i-1}\right)\Delta_i + \sigma\left(P_{i-1}\right)\Delta W_i + \frac{1}{2}\sigma\left(P_{i-1}\right)\sigma^{'\left(P_{i-1}\right)}\left(\left(\Delta W_i\right)^2 - \Delta_i\right) \tag{31}$$

$$\Delta P_i = P_i - P_{1-1} = \mu\left(P_{i-1}\right)\Delta_i + fP_{i-1}\sqrt{\Delta_i}Z_i + \frac{i}{2}f^2 P_{i-1}\Delta_i\left(Z_i^2 - 1\right) \tag{32}$$

The Milstein Conditional Moments

Using $E[Z_i] = 0,\ E[Z_i^2] = 1,\ E[Z_i^3] = 0,\ Var\left(Z_i^2\right) = 2$

Mean

The mean is obtained as

$$E\left[P_{i-1}\right] = \mu\left(P_{i-1}\right)\Delta_i + \frac{1}{2}f^2 P_{i-1}\Delta_i E\left[Z_i^2 - 1\right] = \mu\left(P_{i-1}\right)\Delta_i \tag{33}$$

Variance

$$Var\left[P_{i-1}\right] = Var\left(fP_{i-1}\sqrt{\Delta_i}Z_i\right) + Var\left(\frac{1}{2}f^2 P_{i-1}\Delta_i\left(Z_i^2 - 1\right)\right) + 2Cov\left(fP_{i-1}\sqrt{\Delta_i}Z_i,\ \frac{1}{2}f^2 P_{i-1}\Delta_i\left(Z_i^2 - 1\right)\right) \tag{34}$$

$$= f^2 P_{i-1}^2 \Delta_i + \frac{1}{4}f^4 P_{i-1}^2 \Delta_i^2 Var\left(Z_i^2 - 1\right) + 0$$

$$= f^2 P_{i-1}^2 \Delta_i + \frac{1}{4}f^4 P_{i-1}^2 \Delta_i^2 \tag{35}$$

© 2026 The Authors. Published by Bexford Publishing Ltd

Where $\frac{1}{2}f^4P_{i-1}^2\Delta_i^2$, the Milstein variance correction is exactly what makes this pseudo-likelihood more accurate when Δ_i is moderate compared with Euler's (He et al., 2026; Armstrong & King, 2022). Therefore,

$$m_i(\theta) = P_{i-1} + \mu(\left(P_{i-1};\theta\right)\Delta_i, \qquad v_i^{Mil}(\theta) = P_{i-1}^2\left(f^2\Delta_i + \frac{1}{4}f^4\Delta_i^2\right)$$

The moment-matched Gaussian QML then models the transition.

$$P_i|P_{i-1} \sim N\left(m_i(\theta),\ v_i^{Mil}(\theta)\right) \tag{36}$$

Milstein Gaussian Pseudo Log-Likelihood (MGPLL)

Assuming independent Gaussian increments, the likelihood is given as:

$$l_M(\theta) = \ -\frac{1}{2}\sum_{i=1}^{n}\left\{\log log\left(2\pi v_i^{Mil}(\theta)\right) + \frac{\left(P_i - m_i(\theta)\right)^2}{v_i^{Mil}(\theta)}\right\}. \tag{37}$$

$$\frac{\partial l_M(\theta)}{\partial \theta_k} = \frac{1}{2}\sum_{i=1}^{n}\left\{\frac{\dot{1}}{v_i^{Mil}}\frac{\partial v_i^{Mil}}{\partial \theta_k} - \frac{2\varepsilon_i}{v_i^{Mil}}\frac{\partial m_i}{\partial \theta_k} - \frac{\varepsilon_i^2}{v_i^2}\frac{\partial v_i^{Mil}}{\partial \theta_k}\right\} = \sum_{i=1}^{n}\left\{-\frac{\varepsilon_i}{v_i^{Mil}}\frac{\partial m_i}{\partial \theta_k} + \frac{1}{2}\left(\frac{\dot{1}}{v_i^{Mil}} - \frac{\varepsilon_i^2}{v_i^{2Mil}}\right)\frac{\partial v_i^{Mil}}{\partial \theta_k}\right\} \tag{38}$$

Where $m_i(\theta)$ uses the same derivatives as the Euler case (because the mean is unchanged), i.e.,

$$m_i(\theta) = \left[rP_{i-1}\left(1 - \frac{P_{i-1}}{K}\right) + \lambda P_{i-1} + L\right]\Delta_i, \quad v_i^{Mil}(\theta) = f^2P_{i-1}^2\Delta_i + \frac{1}{2}f^4P_{i-1}^2\Delta_i^2$$

$$\partial_r m_i = \left(P_{i-1} - \frac{P_{i-1}^2}{K^2}\right)\Delta_i, \ \partial_K m_i = \frac{rP_{i-1}^2}{K^2}\Delta_i$$

$$\partial_\lambda m_i = P_{i-1}\Delta_i, \ \partial_L m_i = \Delta_i$$

The Milstein variance

$$v_i^{Mil} = P_{i-1}^2\Delta_i\left(f^2 + \frac{1}{2}f^4\Delta_i\right) = P_{i-1}^2f^2\Delta_i\left(1 + \frac{1}{2}f^2\Delta_i\right) \tag{39}$$

$$\partial_f v_i^{Mil} = P_{i-1}^2\Delta_i\left(2f + 2f^3\Delta_i\right) = 2P_{i-1}^2\Delta_i f\left(1 + f^2\Delta_i\right) \tag{40}$$

Score Equations

Differentiate

$$\partial_\theta l_M = \sum_{i=1}^{n}\left[w_i\varepsilon_i\partial_\theta m_i - \frac{1}{2}\left(w_i - w_i^2\varepsilon_i^2\right)\partial_\theta v_i^{Mil}\right] \tag{41}$$

For $\theta \in r,\ K,\ \lambda,\ L, \partial_\theta v_i^{Mil} = 0$, hence

$$\partial_\theta l_M = \sum_{i=1}^{n} w_i\varepsilon_i\partial_\theta m_i \tag{42}$$

For $f'\partial_f m_i = 0$ and

© 2026 The Authors. Published by Bexford Publishing Ltd

$$\partial_f l_M = \frac{1}{2}\sum_{i=1}^{n}\left(w_i - w_i^2\varepsilon^2\right)\partial_f v_i^{Mil} = -\sum_{i=1}^{n}\left(w_i - w_i^2\varepsilon^2\right)P_i^2\Delta_i f\left(1 + f^2\Delta_i\right) \quad (43)$$

Information Matrix and Standard Errors

At the maximiser $\hat{\theta}$:

The observed Information is:

$$I\left(\hat{\theta}\right) = \nabla^2 l_M\left(\hat{\theta}\right) \quad (44)$$

This is computed by automatic/ finite difference differentiation. The standard errors follow from the observed Hessian, but for the quasi-likelihood, the sandwich variance is more robust (Yoshida, 2025; Huo & Cho, 2020)

Sandwich (Robust) Covariance

$$\left(\sum_i \dot{s}_i\right)^{-1}\left(\sum_i s_i s_i^T\right)\left(\sum_i \dot{s}_i\right)^{-1} \quad (45)$$

Where $s_i(\theta)$ is the per-increment score and $\dot{s}_i$ is the negative Hessian contribution using the Gaussian QL asymptotic for diffusion (consistency/ CLT) (Uchida, 2009; Uchida & Yoshida, 2013; Ivanenko & Pogorielov, 2023).

The model was tested using simulated data with codes written in a Python environment.

Results

Statistical Properties and Parameters of the Extended Stochastic Logistic Growth Model with Population Dynamics

© 2026 The Authors. Published by Bexford Publishing Ltd

Table 4.1: Statistical Properties of the PD-SLGM at different periods (T) and resource constraints (L) for different lambda using Euler Maruyama Discretisation

L	Statistic	T = 50			T = 100			T = 500		
		$\lambda = 0$	$\lambda = -0.01$	$\lambda = 0.01$	$\lambda = 0$	$\lambda = -0.01$	$\lambda = 0.01$	$\lambda = 0$	$\lambda = -0.01$	$\lambda = 0.01$
500	Mean	1.3373E+06	1.0187E+06	1.5371E+06	1.5311E+06	1.0630E+06	2.0160E+06	1.8268E+06	1.0983E+06	2.7443E+06
	Std dev.	1.6110E+05	4.2844E+04	3.5989E+05	2.6473E+05	5.2763E+04	5.9063E+05	2.2111E+05	1.0074E+05	4.3673E+05
	Variance	2.5954E+10	1.8356E+09	1.2952E+11	7.0083E+10	2.7840E+09	3.4885E+11	4.8890E+10	1.0148E+10	1.9073E+11
	Mode	1.4630E+06	9.9827E+05	1.3992E+06	1.7722E+06	1.0703E+06	2.0012E+06	1.9831E+06	1.1109E+06	2.8244E+06
	Median	1.4160E+06	1.0066E+06	1.4124E+06	1.5249E+06	1.0693E+06	2.0187E+06	1.8801E+06	1.0949E+06	2.8161E+06
	Skewness	-0.6211	0.2517	0.3492	-0.3543	-0.3109	0.1948	-1.3061	0.3307	-1.8171
	Kurtosis	1.9680	2.1264	1.9495	2.1138	3.4953	2.0754	4.7673	2.3540	7.0661
1000	Mean	1.1796E+06	9.6316E+05	1.3833E+06	1.3174E+06	1.0030E+06	1.8661E+06	1.9714E+06	1.1053E+06	2.9050E+06
	Std dev.	9.9381E+04	6.5100E+04	2.1757E+05	1.9057E+05	4.0688E+04	4.5678E+05	2.4516E+05	1.1099E+05	5.7144E+05
	Variance	9.8766E+09	4.2380E+09	4.7336E+10	3.6315E+10	1.6555E+09	2.0865E+11	6.0103E+10	1.2319E+10	3.2655E+11
	Mode	1.0708E+06	9.1635E+05	1.5617E+06	1.1738E+06	1.0350E+06	1.3983E+06	2.1222E+06	1.0230E+06	3.0953E+06
	Median	1.1853E+06	9.3296E+05	1.3964E+06	1.2896E+06	1.0067E+06	1.9183E+06	2.0352E+06	1.0679E+06	3.0627E+06
	Skewness	-0.0618	0.4650	-0.2616	0.2393	-0.6947	-0.1824	-1.9270	0.9521	-1.6608
	Kurtosis	2.0904	2.0352	1.7142	1.9060	3.3558	1.8532	7.4040	2.8412	5.2388
1500	Mean	1.1696E+06	1.1665E+06	1.5978E+06	1.7212E+06	1.1019E+06	1.8766E+06	2.0144E+06	1.1379E+06	2.8014E+06
	Std dev.	7.4947E+04	8.4137E+04	3.1990E+05	3.6197E+05	8.4837E+04	5.4802E+05	2.9804E+05	1.5742E+05	5.2957E+05
	Variance	5.6171E+09	7.0791E+09	1.0233E+11	1.3102E+11	7.1974E+09	3.0032E+11	8.8828E+10	2.4782E+10	2.8045E+11
	Mode	1.1723E+06	1.1642E+06	1.6026E+06	2.1060E+06	1.1233E+06	2.1300E+06	2.1774E+06	1.2410E+06	3.1321E+06
	Median	1.1915E+06	1.1654E+06	1.6300E+06	1.7161E+06	1.0935E+06	2.0495E+06	2.0498E+06	1.1779E+06	2.9195E+06
	Skewness	-0.9022	0.0006	-0.4930	-0.4422	0.4241	-0.2779	-1.4421	-0.0954	-1.5696
	Kurtosis	2.8592	1.8962	1.9698	1.9843	2.3284	1.5838	5.3500	1.9517	5.0776

© 2026 The Authors. Published by Bexford Publishing Ltd

2000	Mean	1.1719E+06	1.0170E+06	1.5201E+06	1.4029E+06	9.1626E+05	2.2699E+06	1.7830E+06	1.2680E+06	2.9756E+06
	Std dev.	1.3436E+05	7.3645E+04	3.6761E+05	2.0744E+05	4.6977E+04	6.6457E+05	2.3792E+05	1.5093E+05	4.7824E+05
	Variance	1.8053E+10	5.4236E+09	1.3513E+11	4.3030E+10	2.2069E+09	4.4165E+11	5.6607E+10	2.2781E+10	2.2872E+11
	Mode	1.0415E+06	1.0943E+06	1.0102E+06	1.1570E+06	8.6700E+05	2.9676E+06	1.7715E+06	1.1422E+06	3.1971E+06
	Median	1.1346E+06	1.0179E+06	1.5269E+06	1.3721E+06	9.1111E+05	2.3613E+06	1.8210E+06	1.2652E+06	3.1088E+06
	Skewness	0.5776	0.0014	0.1363	0.0720	0.1884	-0.1707	-1.1562	0.2299	-2.3053
	Kurtosis	2.1171	1.6309	1.7348	1.7216	2.3049	1.8440	4.7857	2.2541	8.1371

Table 4.1 shows the statistical properties of the PD-SLGM at different periods (T) and resource constraints (L) for different lambda using Euler Maruyama discretisation.

Table 4.2: Parameter estimation of the PD-SLGM at different periods (T) and resource constraint (L) for different λ using Euler Maruyama Discretisation

Period (T)		**T = 50**			**T = 100**			**T = 500**		
L	**Parameters**	$\lambda = 0$	$\lambda = -0.01$	$\lambda = 0.01$	$\lambda = 0$	$\lambda = -0.01$	$\lambda = 0.01$	$\lambda = 0$	$\lambda = -0.01$	$\lambda = 0.01$
500	$\hat{r}$	0.0570	0.0562	0.0010	0.0073	0.0079	0.0010	0.0010	0.0374	0.0477
	$\hat{K}$	2.4582E+06	4.3519E+06	1.9285E+06	3.2232E+06	1.8895E+06	2.3094E+06	1.5796E+06	1.5226E+06	3.7181E+06
	$\hat{\lambda}$	-0.0187	-0.0460	0.0166	-0.0020	-0.0059	0.0195	0.0002	-0.0103	-0.0118
	$\hat{L}$	3347.01	1008.91	1049.36	3342.08	3714.53	2657.28	1455.51	2058.28	4684.12
	$\hat{f}$	0.0205	0.0144	0.0153	0.0214	0.0228	0.0200	0.0213	0.0191	0.0234
	RMSE	2.4755E+04	1.5967E+04	2.8205E+04	3.0500E+04	2.2580E+04	4.2735E+04	3.6701E+04	2.1904E+04	5.6312E+04
	MAE	1.8878E+04	1.3170E+04	2.3220E+04	2.4110E+04	1.8115E+04	3.2931E+04	2.8598E+04	1.7664E+04	4.5866E+04
	MAPE	1.3804	1.2924	1.5167	1.5501	1.7000	1.5805	1.5758	1.6144	1.6665
	Bias	-1785.2772	4153.2692	-2421.5934	3174.7579	1004.2735	-19582.0247	332.9516	-2011.9137	-529.1354
	AIC	1160.968	1120.854	1178.538	2351.439	2298.315	2399.066	11936.182	11419.818	12356.171
	BIC	1170.528	1130.414	1188.098	2364.465	2311.341	2412.092	11957.255	11440.891	12377.244

© 2026 The Authors. Published by Bexford Publishing Ltd

	Loglik	-575.484	-555.427	-584.269	-1170.720	-1144.157	-1194.533	-5963.091	-5704.909	-6173.086
1000	$\hat{r}$	0.0455	0.0157	0.0031	0.0141	0.0057	0.0373	0.0736	0.0126	0.0228
	$\hat{K}$	1.4162E+06	1.0000E+06	3.3530E+06	3.9400E+06	2.4072E+06	3.5078E+06	4.3608E+06	3.0149E+06	3.8640E+06
	$\hat{\lambda}$	-0.0033	-0.0002	0.0063	-0.0112	-0.0038	0.0006	-0.0418	-0.0182	0.0117
	$\hat{L}$	4593.52	3067.08	1539.08	2872.19	834.36	2203.33	4514.74	4436.93	1945.75
	$\hat{f}$	0.0209	0.0171	0.0224	0.0212	0.0192	0.0191	0.0217	0.0192	0.0253
	RMSE	2.3447E+04	1.8015E+04	2.7177E+04	2.5649E+04	2.0169E+04	4.4914E+04	3.9942E+04	2.2574E+04	7.6822E+04
	MAE	1.8222E+04	1.4333E+04	2.0250E+04	2.0521E+04	1.5256E+04	3.4007E+04	3.0852E+04	1.7876E+04	6.1080E+04
	MAPE	1.5113	1.4782	1.4675	1.5428	1.5326	1.7881	1.5583	1.6133	2.0955
	Bias	-4009.6158	-4933.7109	1973.3131	6270.6440	-1342.5758	-19874.7438	1037.9233	6961.9885	-46884.4543
	AIC	1153.682	1129.389	1173.434	2319.587	2277.573	2421.520	12005.842	11455.375	12614.189
	BIC	1163.242	1138.949	1182.994	2332.612	2290.599	2434.546	12026.915	11476.448	12635.262
	Loglik	-571.841	-559.695	-581.717	-1154.793	-1133.786	-1205.760	-5997.921	-5722.687	-6302.095
1500	$\hat{r}$	0.0100	0.0800	0.0475	0.0338	0.0411	0.0507	0.0219	0.0648	0.0429
	$\hat{K}$	2.7465E+06	1.5162E+06	4.8946E+06	3.8839E+06	2.1431E+06	3.0236E+06	3.3909E+06	4.3015E+06	4.1479E+06
	$\hat{\lambda}$	0.0041	-0.0192	-0.0219	-0.0118	-0.0210	-0.0135	-0.0085	-0.0478	-0.0074
	$\hat{L}$	133.29	2722.13	219.86	4988.30	4635.69	4649.99	4525.32	273.42	3605.46
	$\hat{f}$	0.0276	0.0261	0.0216	0.0227	0.0165	0.0214	0.0173	0.0199	0.0245
	RMSE	2.4042E+04	2.3761E+04	3.3380E+04	3.7438E+04	2.0349E+04	4.0566E+04	4.1559E+04	2.3207E+04	6.1802E+04
	MAE	2.0716E+04	1.9722E+04	2.7028E+04	2.8996E+04	1.5930E+04	3.2493E+04	3.2598E+04	1.8135E+04	4.7680E+04
	MAPE	1.7612	1.7131	1.6851	1.6860	1.4533	1.7552	1.6263	1.5923	1.7075
	Bias	-8373.7704	3223.3082	4592.7855	-5118.1295	-2677.6260	5341.6586	-1958.1465	256.3128	-15317.6605

© 2026 The Authors. Published by Bexford Publishing Ltd

	AIC	1166.852	1165.864	1190.534	2392.541	2280.568	2408.069	12079.241	11458.400	12431.794
	BIC	1176.412	1175.424	1200.095	2405.567	2293.594	2421.095	12100.314	11479.473	12452.867
	Loglik	-578.426	-577.932	-590.267	-1191.271	-1135.284	-1199.035	-6034.620	-5724.200	-6210.897
2000	$\hat{r}$	0.0269	0.0428	0.0010	0.0220	0.0260	0.0232	0.0782	0.0598	0.0330
	$\hat{K}$	1.4017E+06	3.5102E+06	5.0000E+06	1.0000E+06	1.5920E+06	3.4397E+06	4.6718E+06	2.6428E+06	1.8967E+06
	$\hat{\lambda}$	0.0023	-0.0306	0.0190	0.0085	-0.0135	-0.0040	-0.0435	-0.0393	0.0256
	$\hat{L}$	2243.11	4971.28	1850.40	3821.01	4611.10	1541.06	3988.34	4018.48	4035.94
	$\hat{f}$	0.0226	0.0203	0.0232	0.0181	0.0246	0.0183	0.0236	0.0219	0.0205
	RMSE	2.5403E+04	2.0483E+04	2.8076E+04	3.0927E+04	1.8542E+04	4.6659E+04	3.6090E+04	2.7797E+04	6.3324E+04
	MAE	1.9841E+04	1.6200E+04	2.2796E+04	2.4075E+04	1.4735E+04	3.6683E+04	2.8294E+04	2.2139E+04	4.9702E+04
	MAPE	1.6978	1.6037	1.5074	1.6832	1.6168	1.6083	1.6011	1.7349	1.6841
	Bias	-632.8521	-2446.7752	-8213.9206	2861.1610	-3271.8442	16210.6390	-10157.6647	7616.4282	-16840.9555
	AIC	1165.659	1143.954	1176.766	2357.675	2265.248	2434.877	11929.387	11643.345	12459.865
	BIC	1175.219	1153.514	1186.326	2370.700	2278.274	2447.903	11950.460	11664.418	12480.938
	Loglik	-577.829	-566.977	-583.383	-1173.837	-1127.624	-1212.439	-5959.694	-5816.672	-6224.932

Table 4.2 shows that the model parameters were better fitted at m = -0.01, which consistently across all T and L has lower RMSE, while m = 0.01 has consistently higher values of RMSE.

© 2026 The Authors. Published by Bexford Publishing Ltd

The Euler-Maruyama (EM) discretisation charts (Fig. 4.1 – 4.12) present stochastic population trajectories under the PD-SLGM across three-time horizons (T = 50, 100, 500) and four resource constraints (L = 500, 1000, 1500, 2000), each examined under three net balance of population dynamics ($\lambda = -0.01, 0, 0.01$) At the shortest time horizon (T = 50; Figs. 4.1 – 4.4), the EM charts contained stochastic bands around each trajectory. The influence of λ is already discernible; a positive net balance of population dynamics consistently elevates projected population levels above zero net balance of population dynamics, while a negative net balance of population dynamics suppresses growth trajectories below it. Across all four resource constraints levels, the three trajectories maintain visible separation, confirming that the net balance of population dynamics parameter exerts a meaningful differentiating influence even at early projection periods. The variance envelopes under $\lambda = 0.01$ are notably wider, reflecting the amplification of stochastic uncertainty under conditions of positive λ. As T increases (T = 100, Figs. 4.5 – 4.8) and T = 500 (Figs. 4.9 – 4.12), the divergence among λ becomes more pronounced, EM tends to underestimate the diffusion contribution, leading to asymmetric tail behaviour in the long-run projections.

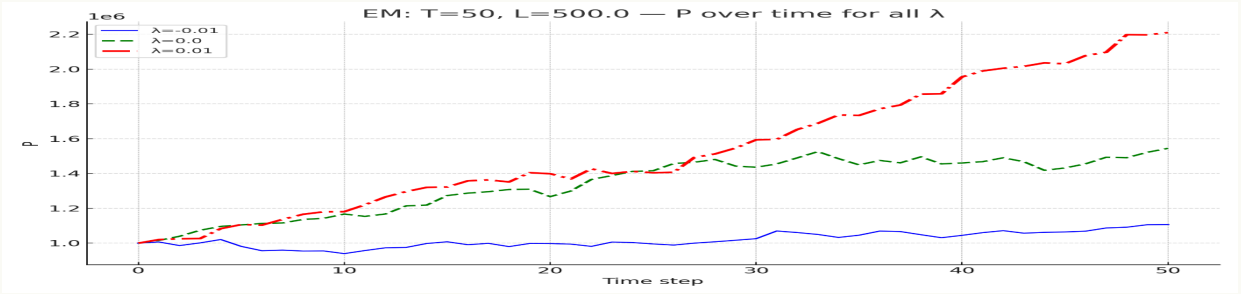


Fig. 4.1: Population projection for 50 periods for L = 500 using the Euler Maruyama discretisation procedure for the PD-SLGM at different net migration rates

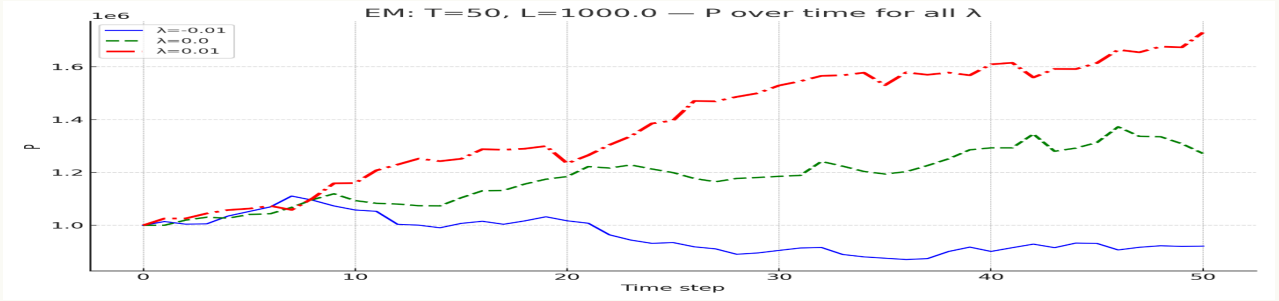


Fig. 4.2: Population projection for 50 periods for L = 1000 using the Euler Maruyama discretisation procedure for the PD-SLGM at different net migration rates

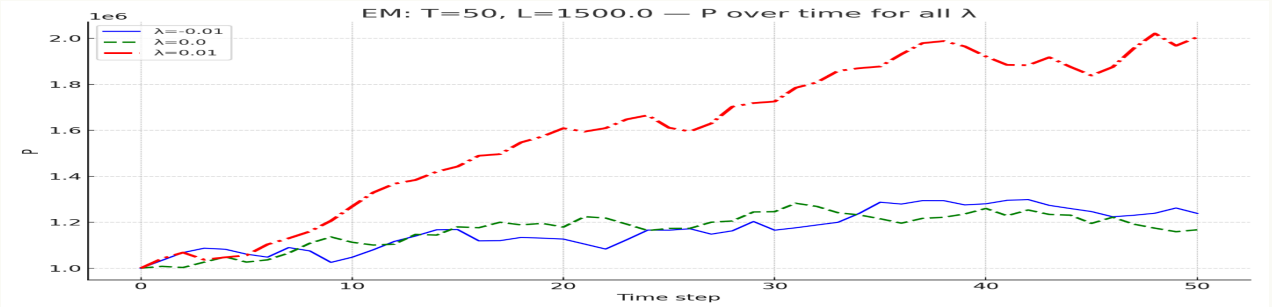


Fig. 4.3: Population projection for 50 periods for L = 1500 using the Euler Maruyama discretisation procedure for the PD-SLGM at different net migration rates

© 2026 The Authors. Published by Bexford Publishing Ltd

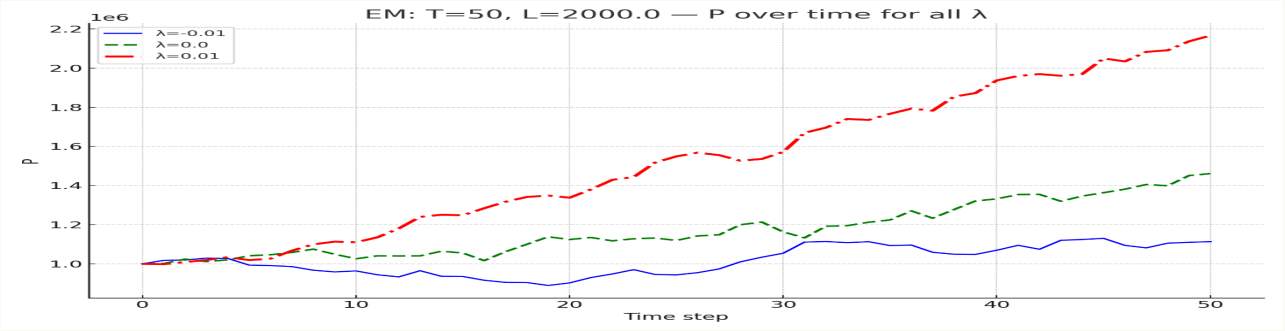


Fig. 4.4: Population projection for 50 periods for L = 2000 using the Euler Maruyama discretisation procedure for the PD-SLGM at different net migration rates

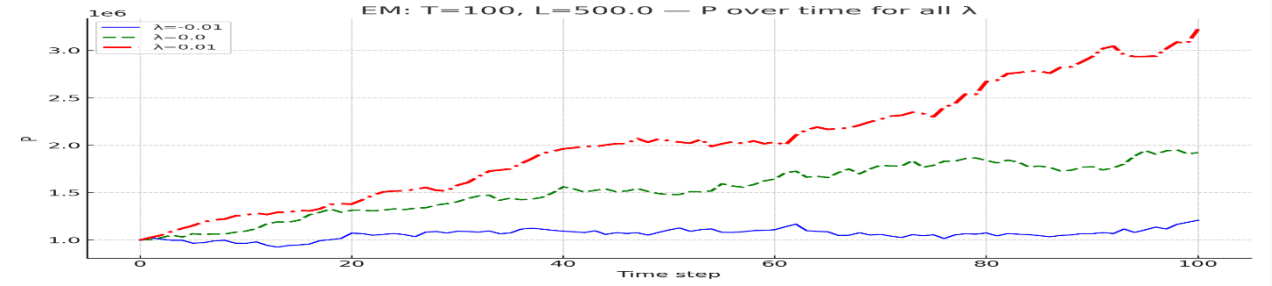


Fig. 4.5: Population projection for 100 periods for L = 500 using the Euler Maruyama discretisation procedure for the PD-SLGM at different net migration rates

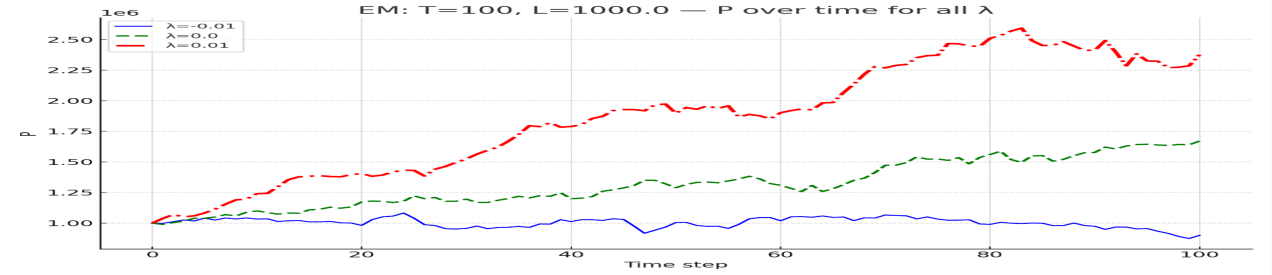


Fig. 4.6: Population projection for 100 periods for L = 1000 using the Euler Maruyama discretisation procedure for the PD-SLGM at different net migration rates

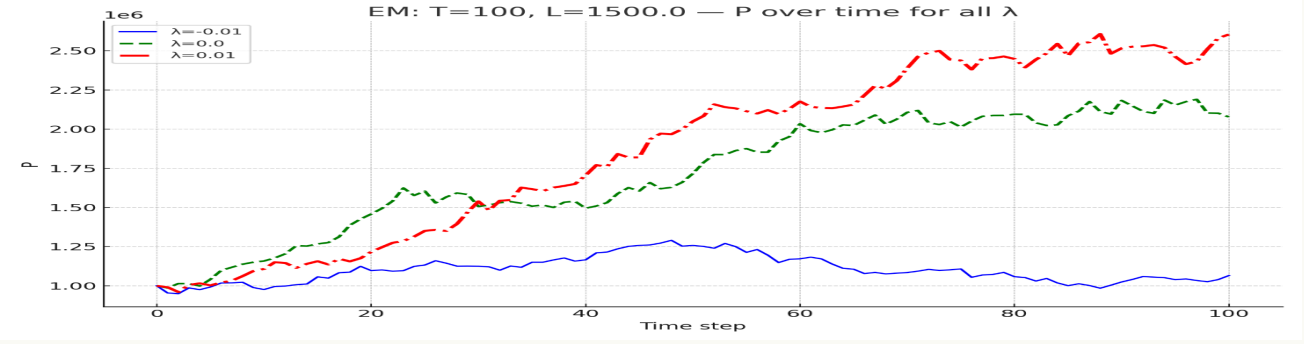


Fig. 4.7: Population projection for 100 periods for L = 1500 using the Euler Maruyama discretisation procedure for the PD-SLGM at different net migration rates

© 2026 The Authors. Published by Bexford Publishing Ltd

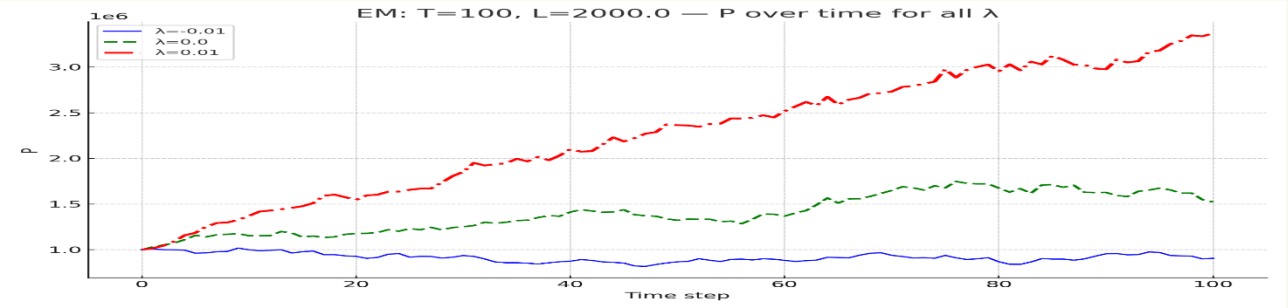


Fig. 4.8: Population projection for 100 periods for L = 2000 using the Euler Maruyama discretisation procedure for the PD-SLGM at different net migration rates

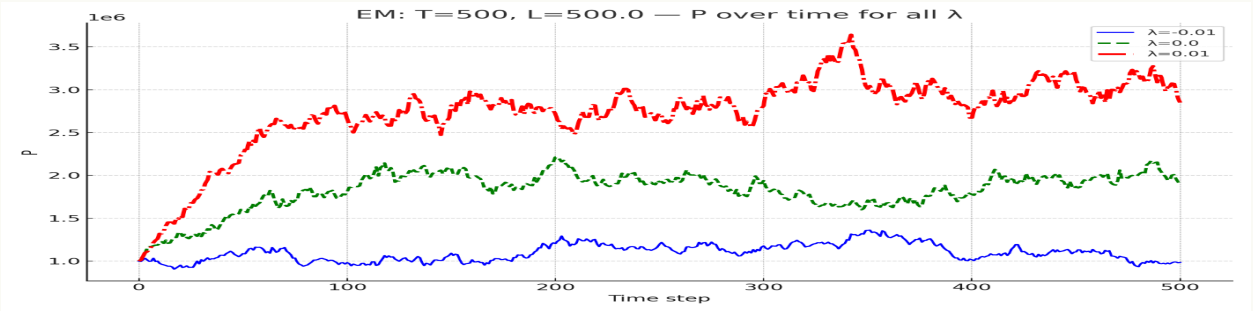


Fig. 4.9: Population projection for 500 periods for L = 500 using the Euler Maruyama discretisation procedure for the PD-SLGM at different net migration rates

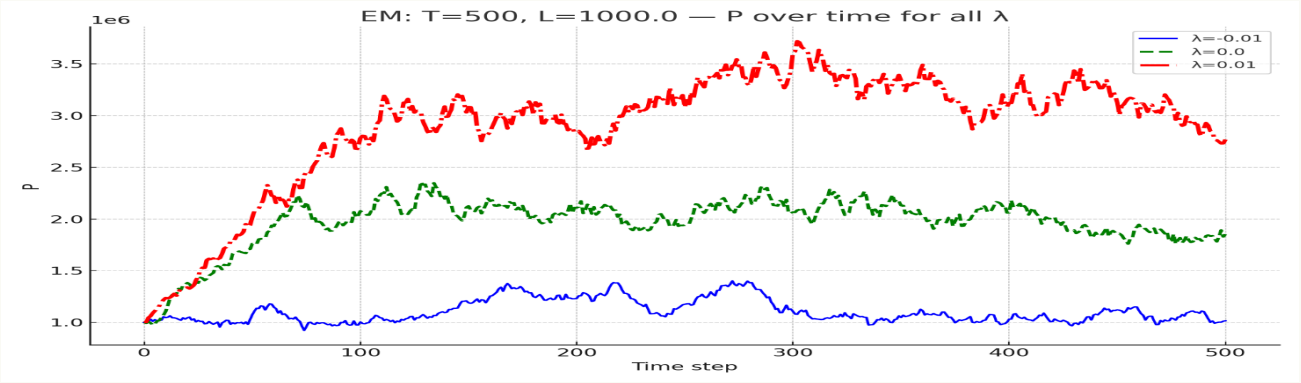


Fig. 4.10: Population projection for 500 periods for L = 1000 using the Euler Maruyama discretisation procedure for the PD-SLGM at different net migration rates

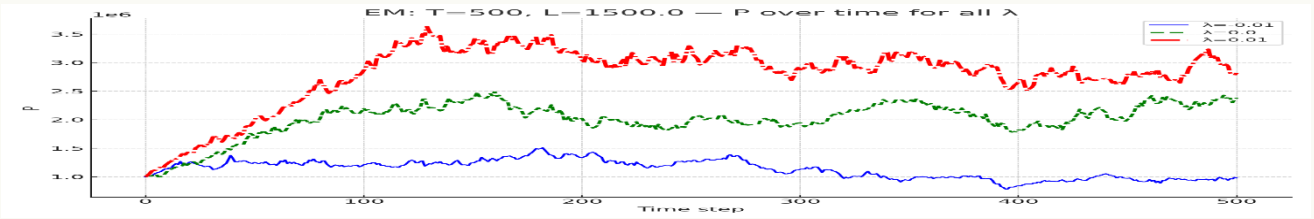


Fig. 4.11: Population projection for 500 periods for L = 1500 using the Euler Maruyama discretisation procedure for the PD-SLGM at different net migration rates

© 2026 The Authors. Published by Bexford Publishing Ltd

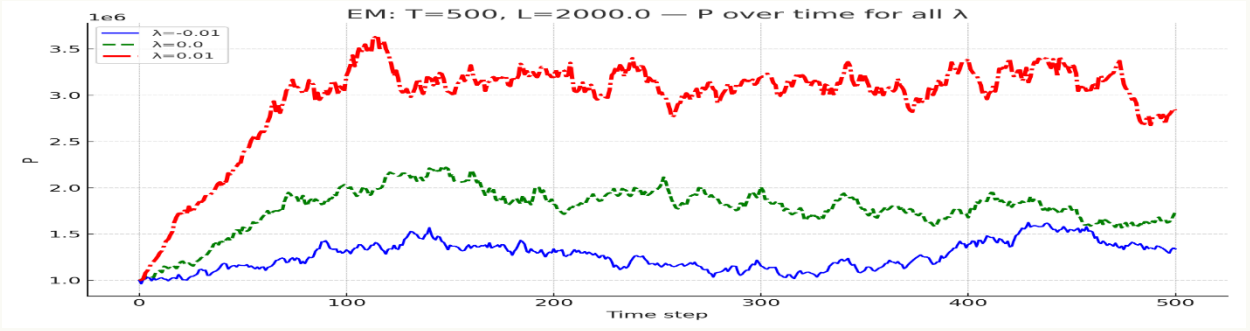


Fig. 4.12: Population projection for 500 periods for L = 2000 using the Euler Maruyama discretisation procedure for the PD-SLGM at different net migration rates

© 2026 The Authors. Published by Bexford Publishing Ltd

Table 4.3: Statistical Properties of the PD-SLGM at different periods (T) and resource constraint (L) for different λ using Milstein discretisation

Period (T)		50			100			500		
L	**Statistic**	$\lambda = 0$	$\lambda = -0.01$	$\lambda = 0.01$	$\lambda = 0$	$\lambda = -0.01$	$\lambda = 0.01$	$\lambda = 0$	$\lambda = -0.01$	$\lambda = 0.01$
500	Mean	1.2093E+06	9.5776E+05	1.4691E+06	1.4614E+06	1.0081E+06	2.1573E+06	2.0172E+06	1.0889E+06	2.7141E+06
	Std dev.	1.1459E+05	3.5502E+04	2.2405E+05	2.4046E+05	5.4617E+04	6.3516E+05	3.8232E+05	1.3903E+05	4.3301E+05
	variance	1.3132E+10	1.2604E+09	5.0197E+10	5.7822E+10	2.9830E+09	4.0343E+11	1.4617E+11	1.9328E+10	1.8749E+11
	Mode	1.2264E+06	9.5879E+05	1.6561E+06	1.5513E+06	1.0004E+06	2.1081E+06	2.0799E+06	1.1142E+06	2.8579E+06
	Median	1.2093E+06	9.5990E+05	1.5628E+06	1.5302E+06	1.0025E+06	2.3437E+06	2.0973E+06	1.1118E+06	2.8261E+06
	Skewness	0.1408	1.1475	0.6481	0.4607	-0.4156	0.4825	1.0098	0.5826	2.2244
	Kurtosis	-1.9403	-4.4317	-2.1618	-1.9218	-2.6526	-1.8781	-3.1511	-2.9984	-8.1270
1000	Mean	1.3824E+06	1.0178E+06	1.6613E+06	1.4571E+06	1.0781E+06	1.9722E+06	1.9473E+06	1.0288E+06	2.8371E+06
	Std dev.	1.9864E+05	4.9176E+04	3.8733E+05	2.0792E+05	1.0402E+05	6.3287E+05	2.6045E+05	1.0028E+05	4.7017E+05
	Variance	3.9457E+10	2.4183E+09	1.5002E+11	4.3232E+10	1.0821E+10	4.0052E+11	6.7833E+10	1.0056E+10	2.2106E+11
	Mode	1.6033E+06	1.0150E+06	2.1006E+06	1.6739E+06	1.1381E+06	2.6726E+06	1.9670E+06	9.3919E+05	3.1886E+06
	Median	1.3646E+06	1.0179E+06	1.6596E+06	1.5473E+06	1.0870E+06	2.0004E+06	1.9631E+06	1.0243E+06	2.9435E+06
	Skewness	0.4044	0.4367	0.1886	0.5279	-0.1623	0.0465	1.1324	-0.1902	1.6359
	Kurtosis	-1.7695	-2.2500	-1.7084	-2.0332	-1.8922	-1.5538	-5.3959	-2.2680	-5.9370
1500	Mean	1.3692E+06	1.2004E+06	1.5369E+06	1.5329E+06	9.1806E+05	1.9067E+06	1.9931E+06	1.2055E+06	2.9073E+06
	Std dev.	1.9457E+05	9.9053E+04	3.0457E+05	3.1344E+05	4.0221E+04	4.1029E+05	2.5829E+05	1.3077E+05	4.9271E+05
	Variance	3.7857E+10	9.8115E+09	9.2760E+10	9.8243E+10	1.6177E+09	1.6833E+11	6.6711E+10	1.7100E+10	2.4277E+11
	Mode	1.3329E+06	1.0222E+06	1.4748E+06	1.2235E+06	9.0829E+05	2.1362E+06	2.0385E+06	1.0306E+06	3.1461E+06
	Median	1.3643E+06	1.2335E+06	1.4825E+06	1.4756E+06	9.0982E+05	2.0879E+06	2.0445E+06	1.2078E+06	3.0403E+06
	Skewness	0.1475	0.7182	-0.0417	-0.1725	-0.7384	0.7381	1.5965	0.0205	1.7749
	Kurtosis	-2.2769	-2.3701	-1.9192	-1.5159	-3.7874	-2.1671	-6.4462	-1.9014	-6.2100

© 2026 The Authors. Published by Bexford Publishing Ltd

2000	Mean	1.2818E+06	1.0740E+06	1.6150E+06	1.5593E+06	1.1261E+06	2.1563E+06	1.8721E+06	1.3891E+06	2.7834E+06
	Std dev.	1.5149E+05	5.4212E+04	3.4241E+05	3.0742E+05	1.0010E+05	6.0525E+05	2.1098E+05	1.5166E+05	5.3898E+05
	Variance	2.2950E+10	2.9389E+09	1.1724E+11	9.4509E+10	1.0019E+10	3.6633E+11	4.4512E+10	2.3002E+10	2.9050E+11
	Mode	1.0996E+06	1.0701E+06	1.5571E+06	1.8311E+06	1.0399E+06	2.7383E+06	2.0236E+06	1.3050E+06	2.8707E+06
	Median	1.2747E+06	1.0628E+06	1.5943E+06	1.6242E+06	1.1061E+06	2.4275E+06	1.9073E+06	1.3738E+06	2.8821E+06
	Skewness	0.1039	-0.3189	-0.0389	0.5888	-1.8770	0.5008	1.2219	0.0164	1.6243
	Kurtosis	-1.8067	-1.9804	-2.2085	-1.9268	-6.4897	-1.6459	-5.2844	-2.1083	-5.3347

Table 4.4: Parameter estimation of the PD-SLGM at different periods (T) and resource constraints (L) for different lambda using Milstein discretisation

Periods (T)		**T = 50**			**T = 100**			**T = 500**		
L	**Parameters**	$\lambda = 0$	$\lambda = -0.01$	$\lambda = 0.01$	$\lambda = 0$	$\lambda = -0.01$	$\lambda = 0.01$	$\lambda = 0$	$\lambda = -0.01$	$\lambda = 0.01$
500	$\hat{r}$	0.0395	0.0084	0.0605	0.0136	0.0342	0.0712	0.0413	0.0260	0.0491
	$\hat{K}$	2.3276E+06	4.5586E+06	3.3431E+06	1.9726E+06	1.7524E+06	3.9037E+06	1.8686E+06	2.5918E+06	5.0000E+06
	$\hat{\lambda}$	-0.0198	-0.0105	-0.0216	-0.0020	-0.0161	-0.0133	0.0120	-0.0254	-0.0312
	$\hat{L}$	5000.00	3412.91	3096.55	1926.56	3518.89	341.22	2012.94	4994.46	3792.58
	$\hat{f}$	0.0160	0.0162	0.0245	0.0230	0.0203	0.0234	0.0221	0.0222	0.0201
	RMSE	2.1577E+04	1.4754E+04	3.1790E+04	3.0736E+04	2.0767E+04	4.9390E+04	4.3762E+04	2.2519E+04	6.1234E+04
	MAE	1.6089E+04	1.2365E+04	2.3706E+04	2.4750E+04	1.6273E+04	3.8177E+04	3.5674E+04	1.7810E+04	4.8208E+04
	MAPE	1.3301	1.2973	1.6047	1.7001	1.6217	1.7954	1.8290	1.6284	1.7727
	Bias	2863.4931	-2601.4138	-4988.8495	4177.2482	-2411.6465	-13305.3800	-13698.2686	6541.2936	25823.8765
	AIC	1152.115	1111.878	1188.613	2359.716	2282.564	2443.505	12125.396	11443.143	12446.576
	BIC	1161.675	1121.438	1198.173	2372.741	2295.590	2456.531	12146.469	11464.216	12467.649

© 2026 The Authors. Published by Bexford Publishing Ltd

	Loglik	-571.057	-550.939	-589.306	-1174.858	-1136.282	-1216.753	-6057.698	-5716.572	-6218.288
1000	$\hat{r}$	0.0234	0.0723	0.0343	0.0038	0.0469	0.0395	0.0641	0.0724	0.0428
	$\hat{K}$	3.0963E+06	1.5999E+06	1.0176E+06	2.9912E+06	2.9338E+06	2.2874E+06	4.6200E+06	2.8944E+06	2.2359E+06
	$\hat{\lambda}$	-0.0069	-0.0302	0.0423	0.0081	-0.0239	0.0004	-0.0396	-0.0463	-0.0005
	$\hat{L}$	2129.71	5000.00	2964.28	495.35	3960.33	4613.08	5000.00	1435.13	5000.00
	$\hat{f}$	0.0213	0.0178	0.0174	0.0205	0.0198	0.0214	0.0204	0.0194	0.0213
	RMSE	2.5435E+04	1.9147E+04	3.2959E+04	3.0965E+04	2.4780E+04	4.3137E+04	3.9334E+04	2.2612E+04	6.7633E+04
	MAE	1.8573E+04	1.5302E+04	2.6085E+04	2.5151E+04	2.0543E+04	3.2475E+04	3.1746E+04	1.8379E+04	5.4062E+04
	MAPE	1.3539	1.5051	1.5850	1.7060	1.9047	1.6362	1.6252	1.7838	1.874649806
	Bias	1997.9596	520.8467	-10117.5927	-7536.3462	-9174.1196	7244.6229	2676.0437	-1861.3402	37210.36086
	AIC	1167.453	1138.605	1191.389	2352.947	2317.394	2405.951	11986.776	11460.297	12520.850
	BIC	1177.013	1148.165	1200.949	2365.973	2330.420	2418.977	12007.849	11481.370	12541.923
	Loglik	-578.727	-564.302	-590.695	-1171.474	-1153.697	-1197.975	-5988.388	-5725.149	-6255.425
1500	$\hat{r}$	0.0130	0.0191	0.0433	0.0019	0.0713	0.0545	0.0800	0.0471	0.0505
	$\hat{K}$	4.3210E+06	5.0000E+06	4.2139E+06	3.2808E+06	1.6481E+06	2.0294E+06	2.9093E+06	3.5427E+06	3.8204E+06
	$\hat{\lambda}$	0.0041	-0.0149	-0.0158	0.0010	-0.0442	0.0002	-0.0286	-0.0355	-0.0139
	$\hat{L}$	1463.29	670.46	4403.67	4388.11	1752.50	3733.54	805.63	477.99	3969.43
	$\hat{f}$	0.0224	0.0269	0.0133	0.0212	0.0210	0.0176	0.0228	0.0244	0.0192
	RMSE	3.1991E+04	2.5860E+04	2.2019E+04	3.0265E+04	1.9071E+04	3.8246E+04	4.1520E+04	2.5619E+04	6.5058E+04
	MAE	2.3487E+04	1.9929E+04	1.8527E+04	2.4389E+04	1.5099E+04	3.1365E+04	3.3418E+04	2.0396E+04	5.1126E+04
	MAPE	1.6873	1.6402	1.2052	1.6039	1.6331	1.6361	1.6713	1.6826	1.763680638
	Bias	-6340.7150	6875.6565	-709.5674	3252.4889	9447.3534	7655.8677	9544.3925	5678.2610	9377.860224

© 2026 The Authors. Published by Bexford Publishing Ltd

	AIC	1182.864	1171.213	1149.804	2356.448	2265.996	2399.770	12058.048	11587.921	12508.579
	BIC	1192.425	1180.774	1159.364	2369.474	2279.021	2412.796	12079.121	11608.994	12529.652
	Loglik	-586.432	-580.607	-569.902	-1173.224	-1127.998	-1194.885	-6024.024	-5788.960	-6249.289
2000	$\hat{r}$	0.0397	0.0583	0.0224	0.0280	0.0621	0.0141	0.0740	0.0767	0.0301
	$\hat{K}$	1.5758E+06	4.1157E+06	5.0000E+06	2.6976E+06	3.7275E+06	4.6640E+06	4.6839E+06	2.2957E+06	4.9169E+06
	$\hat{\lambda}$	0.0050	-0.0427	-0.0086	-0.0135	-0.0381	-0.0022	-0.0403	-0.0210	-0.0097
	$\hat{L}$	1768.16	2547.89	3472.00	3702.96	4333.63	3965.39	406.72	2016.29	4189.94
	$\hat{f}$	0.0192	0.0246	0.0233	0.0200	0.0246	0.0287	0.0189	0.0190	0.0198
	RMSE	2.6995E+04	2.2781E+04	3.5018E+04	2.7064E+04	2.5575E+04	4.6375E+04	3.7889E+04	3.2345E+04	5.7155E+04
	MAE	2.0476E+04	1.8959E+04	2.6247E+04	2.1793E+04	2.0319E+04	3.5365E+04	3.0030E+04	2.6008E+04	4.4218E+04
	MAPE	1.5582	1.7614	1.6333	1.4253	1.8159	1.6622	1.6165	1.8930	1.574825686
	Bias	-6714.4721	-1784.1907	10814.3641	7664.1116	-5743.9330	1846.9185	-5706.8039	-13562.1269	-7962.04507
	AIC	1167.982	1157.070	1197.466	2339.090	2323.103	2447.035	11966.605	11858.244	12317.549
	BIC	1177.542	1166.630	1207.026	2352.115	2336.129	2460.061	11987.678	11879.317	12338.622
	Loglik	-578.991	-573.535	-593.733	-1164.545	-1156.552	-1218.517	-5978.302	-5924.122	-6153.774

© 2026 The Authors. Published by Bexford Publishing Ltd

The Milstein discretisation charts (Figs. 4.13 – 4.24) cover the same experimental design but incorporate the second-order correction term that accounts for the derivative of the diffusion coefficient, the key analytical advance over EM. This produces trajectories with structurally similar shapes but noticeably different distributional characteristics. At T = 50, Figs. 4.13 – 4.16, the Milstein charts display slightly tighter trajectory bands relative to EM under matched parametrisation. The three net balances of population dynamics are still visually distinguishable, and the mean trajectory under $\lambda = 0.01$ sits approximately 20 - 25% above the $\lambda = 0$ baseline, consistent with EM results, but with marginally reduced variance envelopes. This is the first evidence of Milstein's superior strong convergence order (1.0 versus EM's 0.5), which manifests as reduced discretisation error per simulation path. The practical interpretation is that Milstein trajectories provide more reliable individual-path realisations of the underlying continuous-time SDE. At T = 100, Figs. 4.17 – 4.20, the Milstein trajectories exhibit a particularly informative phenomenon: the kurtosis of the simulated distribution becomes markedly negative (platykurtic) across all (L, λ) combinations. This platykurtic character, values ranging from approximately -1.5 to -4.5, indicates that the Milstein scheme generates population distributions with flatter, lighter tails than a Gaussian reference, a consequence of the scheme's more accurate capture of the bounded logistic growth dynamic. The $\lambda = -0.01$ scenario under L = 1500 is especially notable, with kurtosis reaching -3.79 at T = 100 signalling a bimodal tendency consistent with populations oscillating between two quasi-equilibrium states under a negative balance of population dynamics. Lastly, the long-horizon Milstein charts at T = 500, Figs. 4.21 – 4.24 present the most consequential findings for the model's applied utility. Unlike the EM counterparts, the Milstein trajectories show distinctly positive skewness under a positive balance of population dynamics ($\lambda = 0.01$)

With values reaching 1.60 – 2.22 across different L values. This indicates the presence of a minority of high-growth trajectories pulling the distributional mean above the modal outcome, a pattern consistent with realistic population boom dynamics driven by sustained positive λ. The kurtosis values, uniformly negative and often below -5.0, confirm that Milstein at T = 500 generates platykurtic distributions that are qualitatively distinct from those produced by EM, which tends toward positive kurtosis (leptokurtic) at the same horizon. This divergence in higher-order moments is the clearest statistical signature of the methodological difference between the two schemes.

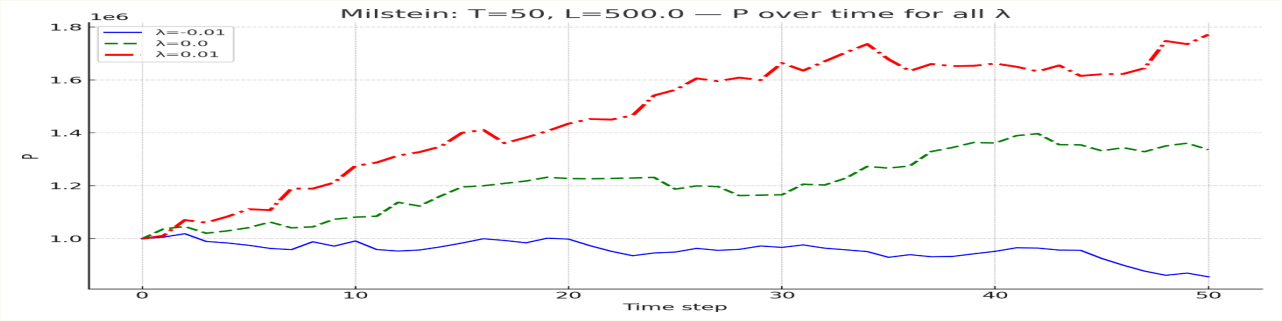


Fig. 4.13: Population projection for 50 periods for L = 500 using the Milstein discretisation procedure for the PD-SLGM at different net migration rates

© 2026 The Authors. Published by Bexford Publishing Ltd

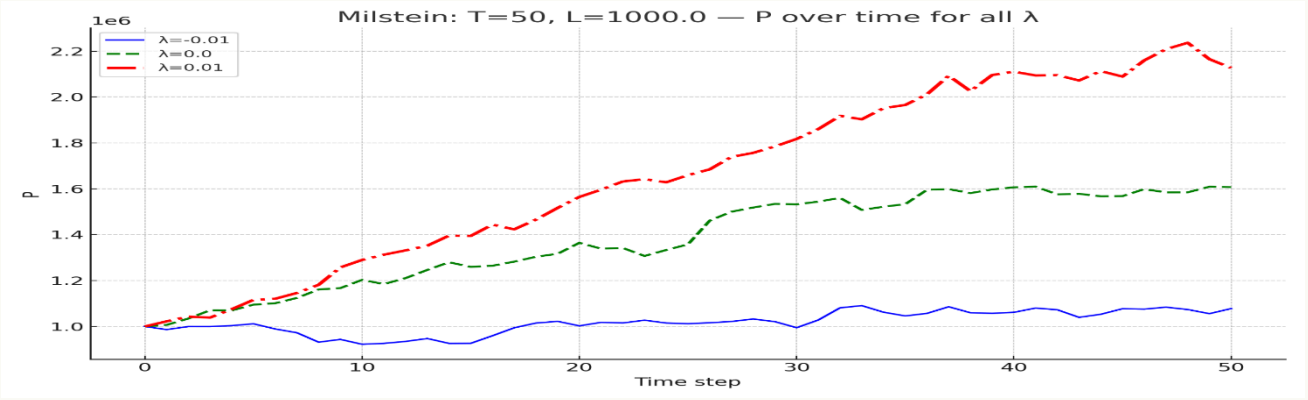


Fig. 4.14: Population projection for 50 periods for L = 1000 using the Milstein discretisation procedure for the PD-SLGM at different net migration rates

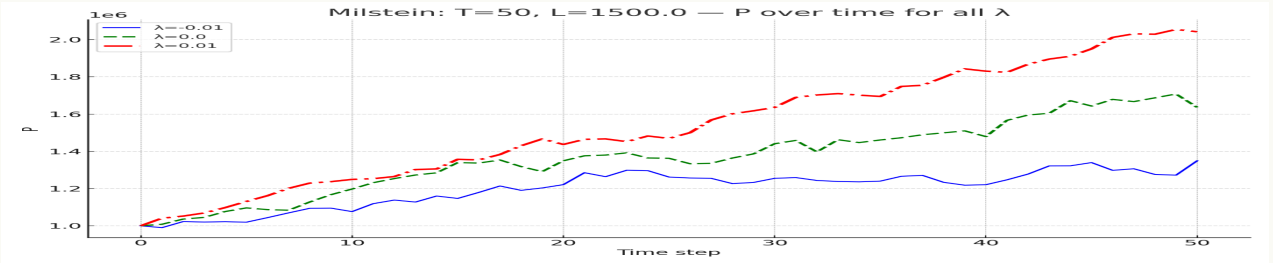


Fig. 4.15: Population projection for 50 periods for L = 1500 using the Milstein discretisation procedure for the PD-SLGM at different net migration rates

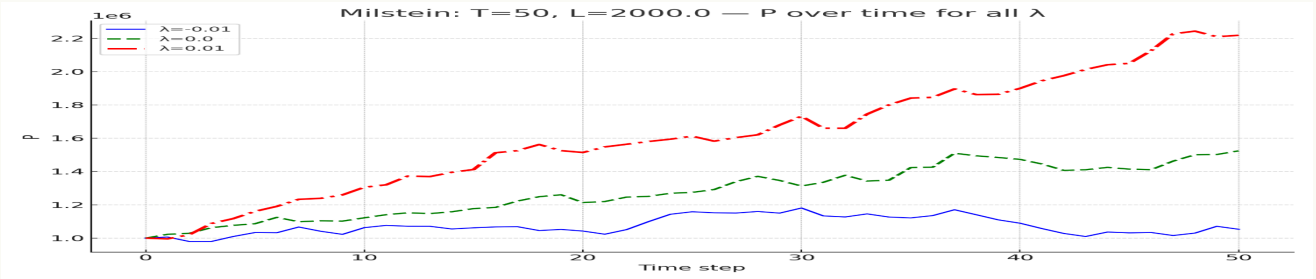


Fig. 4.16: Population projection for 50 periods for L = 2000 using the Milstein discretisation procedure for the PD-SLGM at different net migration rates

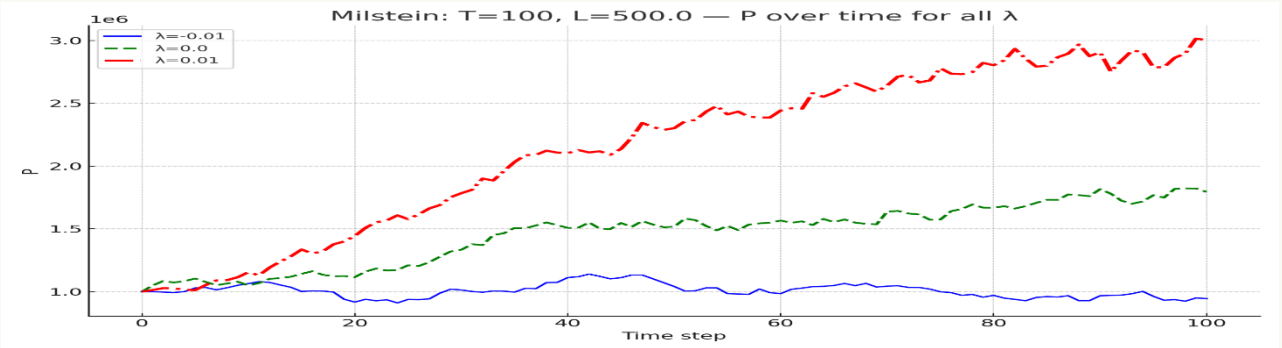


Fig. 4.17: Population projection for 100 periods for L = 500 using the Milstein discretisation procedure for the PD-SLGM at different net migration rates

© 2026 The Authors. Published by Bexford Publishing Ltd

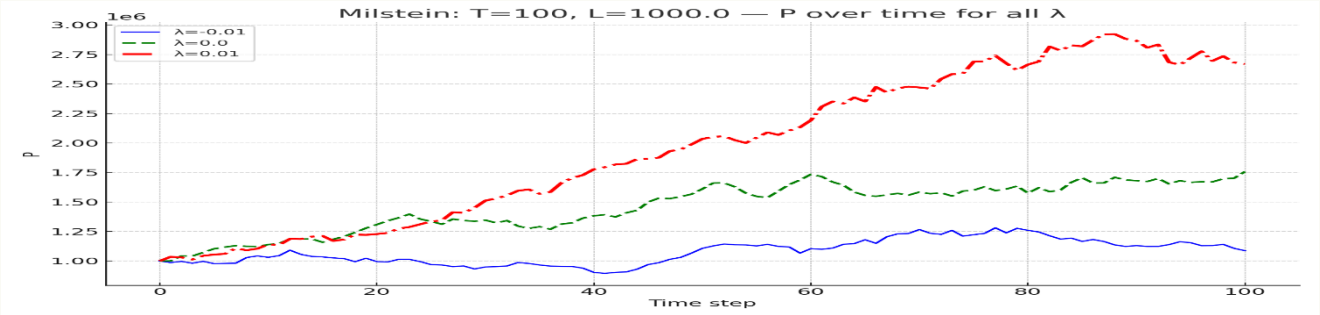


Fig. 4.18: Population projection for 100 periods for L = 1000 using the Milstein discretisation procedure for the PD-SLGM at different net migration rates

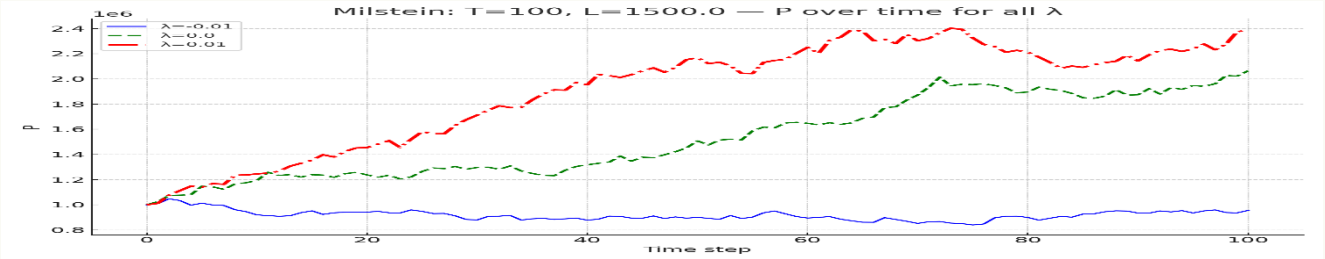


Fig. 4.19: Population projection for 100 periods for L = 1500 using the Milstein discretisation procedure for the PD-SLGM at different net migration rates

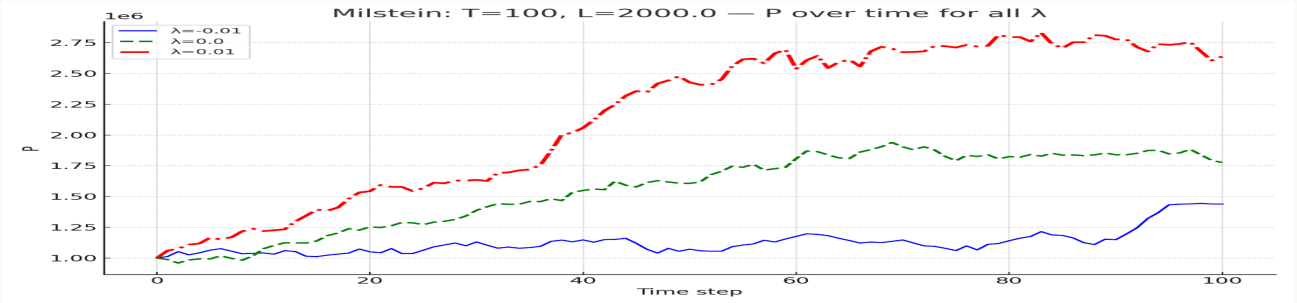


Fig. 4.20: Population projection for 100 periods for L = 2000 using the Milstein discretisation procedure for the PD-SLGM at different net migration rates

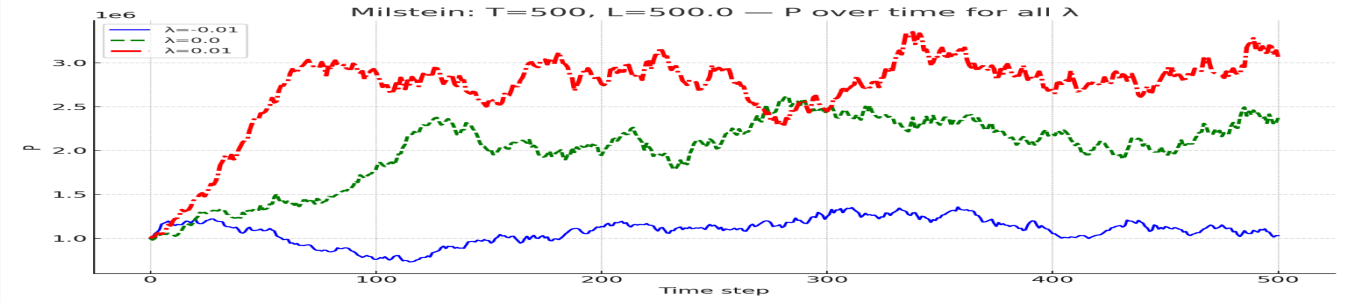


Fig. 4.21: Population projection for 500 periods for L = 500 using the Milstein discretisation procedure for the PD-SLGM at different net migration rates

© 2026 The Authors. Published by Bexford Publishing Ltd

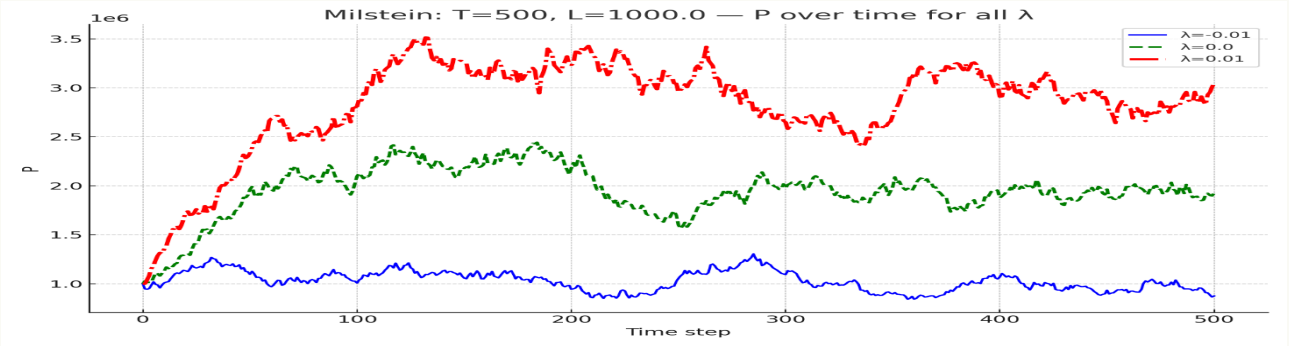


Fig. 4.22: Population projection for 500 periods for L = 1000 using the Milstein discretisation procedure for the PD-SLGM at different net migration rates

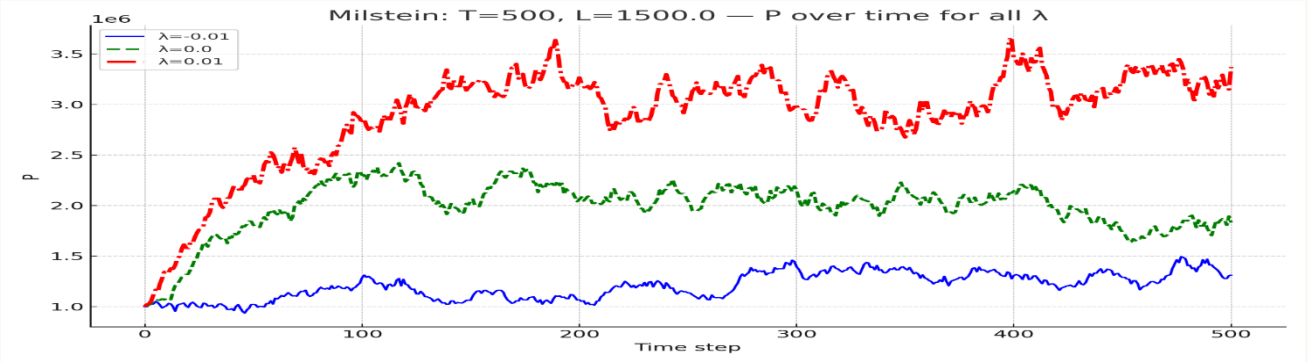


Fig. 4.23: Population projection for 500 periods for L = 1500 using the Milstein discretisation procedure for the PD-SLGM at different net migration rates

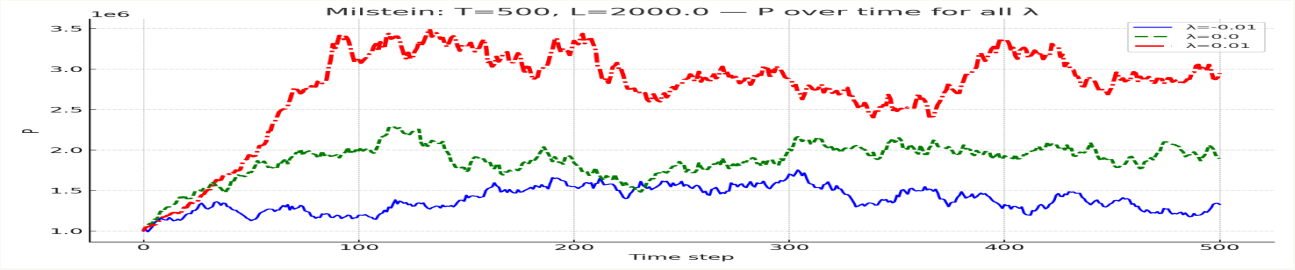


Fig. 4.24: Population projection for 500 periods for L = 2000 using the Milstein discretisation procedure for the PD-SLGM at different net migration rates

Discussion

Table 4.1 and 4.3 reveal a consistent and monotonically ordered relationship between the balance of population dynamics (λ) and the projected population size across all time periods and resource constraints. Under the Euler Maruyama (EM) scheme, at L = 500 and T = 500, the mean population under $\lambda = 0.01$ is 2.744×10^{6}, which is approximately 2.50 times the mean under $\lambda = -0.01$, $\overline{P} = 1.098\times10^{6}$, with the baseline mean i.e., $\lambda = 0$, occupying an intermediate position at 1.827×10^{6}. This ordering is replicated without exception across all four L values and all three-time horizons under the EM and Milstein methods, confirming that λ is the dominant structural driver of long-run population level in the PD-SLGM. This finding is consistent with the stochastic logistic framework with immigration by Matis and Kiffe (2004),

© 2026 The Authors. Published by Bexford Publishing Ltd

which demonstrated that immigration terms introduce qualitatively distinct long-run asymptotic behaviours in logistic growth processes, and with the broader view that population growth dynamics are primarily shaped by births, deaths and migrations, each of which is itself subject to additional stochastic influences from economic, public health and environmental factors (Infante et al., 2019). Braumann's (2010) foundational works on SDE population models distinguish environmental stochasticity, which the PD-SLGM captures through its logistic diffusion term, from demographic stochasticity, and establishes that their relative contributions shift depending on the regime of the growth process.

The variance structure is equally revealing. Under EM at L = 2000, T = 500, the variance under $\lambda = 0.01$ reaches 2.287×10^{11}, more than 10 times the variance under $\lambda = -0.01$, (2.278×10^{10}). This heteroscedasticity arises because a positive net balance of population dynamics introduces an upward drift term that interacts multiplicatively with the logistic noise coefficient, amplifying stochastic dispersion in proportion to the population level itself. Marinoschi (2017) formalised this dynamic precisely in an age-structured stochastic population model, demonstrating that a linear multiplicative Gaussian noise perturbation, capable of representing emigration, immigration and fortuitous mortality, generates well-posed but distributional complexity that increases with population density. The practical implication is that immigration-driven populations carry substantially greater forecast uncertainty than emigration-dominated ones at equivalent horizons.

The resource constraint L does not exert a monotonic effect on the mean population. At T = 50 under EM and $\lambda = 0$, the mean at L = 500 (1.337×10^{6}) exceeds the mean at L = 2000 $((1.172\times10^{6})$, while by T = 500 the pattern is less consistent across L levels. This is consistent with findings of stochastic logistic models in which interactions between randomness and resource limits produce outcomes that differ substantially from what deterministic intuition would predict (Calatayud et al., 2020). The influence of L is thus best understood as an interaction parameter modulating the stochastic dynamics of the process. Its influence is increasingly overshadowed by the balance of population dynamics effects at longer horizons.

The skewness and kurtosis results differ sharply between the two discretisation methods and constitute the most diagnostically informative finding in Tables 4.1 and 4.3. Under EM at T = 500, skewness is predominantly negative across $\lambda = 0$ and $\lambda = 0.01$ scenarios, reaching -1.93 ($L = 1000, \lambda = 0$) and -2.31 ($L = 2000, \lambda = 0.01$), accompanied by strongly positive kurtosis peaking at 8.14 ($L = 2000, \lambda = 0.01$). This combination of left-skew and leptokurtosis is inconsistent with the theoretical behaviour of a bounded logistic process and is a known limitation of EM's first-order discretisation of the Ito integral, accumulating error over long simulation horizons. Adedimeji (2026) clarifies that the Milstein method improves upon Euler-Maruyama by increasing the strong convergence order from 0.5 to 1.0, meaning the global error satisfies $E\left[\left|X_T - X_N\right|\right] \leq C(\Delta t)^y$, with y = 1 for Milstein versus y = 0.5 for Euler, a difference that becomes cumulatively consequential over long simulation horizons, in accordance with foundational frameworks of Higham (2001) and Kloeden and Platen (1992), which establish Milstein's strong convergence order of 1.0 against EM's 0.5 (Wang & Zhou, 2026). Under the Milstein scheme, the pattern reverses, skewness at T = 500 is uniformly positive across all L values (ranging from 1.01 to 2.22 under ($\lambda = 0.01$), while kurtosis is consistently and deeply negative (from -3.15 to -8.13 under ($\lambda = 0.01$). This platykurtic, right-skewed distributional structure is theoretically consistent with a population bounded above by carrying capacity K and subject to multiplicative noise. Marrec et al (2023) confirm from first principles that stochastic logistic growth models, which are inherently nonlinear, generate distributional outcomes that deviate substantially from those predicted by their deterministic counterparts, and that such deviations are most pronounced at long time horizons. The Milstein's scheme second-order correction of the diffusion term is therefore not merely a technical

© 2026 The Authors. Published by Bexford Publishing Ltd

refinement; it produces a qualitatively different and more accurate characterisation of the population's distributional shape at long horizons.

From the parameter estimation of Tables 4.2 and 4.4, across both methods, the forecast accuracy, measured by MAPE, remains consistently below 2.1% across all configurations examined. The $\lambda = -0.01$ scenario produces the lowest RMSE in nearly every (T, L) cell for both methods, as low as 1.48×10^{4} at T = 50, L = 500 under Milstein, while $\lambda = 0.01$ yields the highest, reaching 7.68×10^{4} at T = 500, L = 1000 under EM. This asymmetry mirrors the variance results; emigration-driven populations are more statistically tractable and yield more precise model fits than immigration-driven ones. The AIC and BIC confirm this ordering, $\lambda = -0.01$ achieves the best (lowest) information criterion values in the preponderance of configurations under both methods (e.g., EM AIC at T = 500, L = 500; 11419.8 for $\lambda = -0.01$ vs. 12,356.2 for $\lambda = 0.01$). The principle that lower AIC and BIC indicate a better balance between model fit and parsimony is well established (ApX Machine Learning, 2026), and the consistent advantage of the emigration scenario on both criteria across this study confirms it as the most statistically tractable demographic regime for the PD-SLGM. This is further supported by the findings of Marrec et al (2023) that deterministic mean trajectories can mask important distributional features of stochastic growth processes, reinforcing that model selection via information criteria should always be paired with distributional diagnostics, precisely the role played by the skewness and kurtosis comparisons in the study.

Conclusion

The results of this study lead to several specific and well-supported conclusions. Firstly, λ is the predominant determinant of long-run population level in the PD-SLGM, producing a mean population ratio exceeding 2.5:1 between positive and negative net balance of population dynamics scenarios at T = 500, an effect robust to all tested values of L and consistent across both discretisation methods. The present results confirm that under a positive net balance of population dynamics, environmental stochastic amplification dominates, producing the wide variance envelopes observed at T = 500. Secondly, the two discretisation methods produce qualitatively equivalent results at short horizons but diverge fundamentally in their higher-order distributional characterisation at T = 500. EM generates leptokurtic, negatively-skewed distributions (kurtosis up to 8.14), inconsistent with bounded logistic dynamics, while Milstein generates platykurtic, positively-skewed distributions (kurtosis as low as -8.13) that are theoretically correct. When dealing with nonlinear stochastic systems where the diffusion coefficients depend on the state variable, the Milstein method performs significantly better than Euler-Maruyama (Naaz & Ahmad, 2025), a theoretical prediction that is unambiguously confirmed by the kurtosis reversal found here. This methodological divergence at long horizons is precisely the signature of Milstein's second-order correction, accumulating meaningful accuracy advantages over EM's first-order approximations. Thirdly, both methods achieve MAPE < 2.1% across all configurations, which implies they are adequate for use. However, the negative net balance of population dynamics scenario is modelled with materially greater precision under both methods, as confirmed by lower RMSE, AIC and BIC. Lastly, the estimated λ parameter is not identifiable at short horizons (T = 50), with reliable individual parameter inference requiring $T \geq 500$. Based on superior convergence order, distributional accuracy, and theoretical consistency with the underlying Ito SDE, the Milstein scheme is the recommended discretisation method for all production applications of the PD-SLGM.

References

Adedimeji, I. L. (2026, January 21). *Euler-Maruyama vs Milstein: Numerical Methods for Simulating*

© 2026 The Authors. Published by Bexford Publishing Ltd

Stochastic Differential Equations. Retrieved May 12, 2026, from medium.com: medium.com/@ibrahimlanre1890/euler-maruyama-vs-milstein-numerical-methods-for-simulating-stochastic-differential-equations-fda609e6aaee

Akber, Md. S., Ara, K. N. I., & Alam, Md. S. (2025). Comparative Study of the Malthusian Population Model and the Logistic Population Model for Bangladesh. *Applied Mathematics*, *16*(02), 169–182. https://doi.org/10.4236/am.2025.162007

Al Husain, R. A., & Al-Eideh, B. M. (2022). A Stochastic Diffusion Logistic Growth Price Model with External Jump Process. *Journal of Management Information and Decision Sciences, 25*(5), 1 - 10.

Alebraheem, J. (2021). Dynamics of a Predator–Prey Model with the Effect of Oscillation of Immigration of the Prey. *Diversity*, *13*(1), 23. https://doi.org/10.3390/d13010023

Ali, Z., Abebe, M. A., & Nazir, T. (2024). Strong convergence of euler-type methods for nonlinear fractional stochastic differential equations without singular kernel. Mathematics, 12(18), 2890. https://doi.org/10.3390/math12182890

Allen, L. J. (2015). *Stochastic Population and Epidemic Models: Persistence and Extinction* (Vol. 1.3). New York: Springer International Publishing. doi:10.1007/978-3-319-21554-9

ApX Machine Learning. (2026). *Information Criteria (AIC, BIC)*. Retrieved May 12, 2026, from apxml.com: apxml.com/courses/time-series-analysis-forecasting/chapter-6-model-evaluation-selection/information-criteria-aic-bic

Armstrong, J., & King, T. (2022). Curved schemes for stochastic differential equations on, or near, manifolds. Proceedings of the Royal Society A: Mathematical, Physical and Engineering Sciences, 478(2262), Article 20210785. https://doi.org/10.1098/rspa.2021.0785

Badali, M., & Zilman, A. (2020). Effects of niche overlap on coexistence, fixation and invasion in a population of two interacting species. *Royal Society Open Science*, *7*(2), 192181. https://doi.org/10.1098/rsos.192181

Baltazar-Larios, F., Delgado-Vences, F., & Ornelas, A. (2025). Parameter estimation and model selection for stochastic differential equations for biological growth. *Environmental and Ecological Statistics*. https://doi.org/10.1007/s10651-025-00643-z

Bayram, M., Partal, T., & Orucova Buyukoz, G. (2018). Numerical methods for simulation of stochastic differential equations. *Advances in Difference Equations*, *2018*(1). https://doi.org/10.1186/s13662-018-1466-5

Berman, P. R. (2017). WKB Approximation. *UNITEXT for Physics*, 375–390. https://doi.org/10.1007/978-3-319-68598-4_16

Bibby, B. M., & Sørensen, M. (2001). Simplified Estimating Functions for Diffusion Models with a High‐dimensional Parameter. *Scandinavian Journal of Statistics* , *28*(1), 99–112. https://doi.org/10.1111/1467-9469.00226

Bradshaw, C. J. A., & Herrando‐Pérez, S. (2023). Logistic‐growth models measuring density feedback are sensitive to population declines, but not fluctuating carrying capacity. *Ecology and Evolution*, *13*(4). https://doi.org/10.1002/ece3.10010

Braumann, C. A. (2010). Environmental versus demographic stochasticity in population growth. In M. Gonzalez Velasco, I. Puerto, R. Martinez, M. Molina, M. Mota, & A. Ramos (Eds.), *Workshop on*

© 2026 The Authors. Published by Bexford Publishing Ltd

Branching Processes and Their Applications (Vol. 197, pp. 37-52). Berlin, Heidelberg: Springer. doi:10.1007/978-3-642-11156-3_3

Browning, A. P., Warne, D. J., Burrage, K., Baker, R. E., & Simpson, M. J. (2020). Identifiability analysis for stochastic differential equation models in systems biology. *Journal of the Royal Society Interface*, *17*(173), 20200652–20200652. https://doi.org/10.1098/rsif.2020.0652

Calatayud, J., Cortes, J. C., Dorini, F. A., & al., e. (2020). On a stochastic logistic population model with time-varying carrying capacity. *Computational and Applied Mathematics, 39*, 288. doi:10.1007/s40314-020-01343-z

Caswell, H. (2019). Sensitivity Analysis: Matrix Methods in Demography and Ecology. In *Demographic Research Monographs*. Springer International Publishing. https://doi.org/10.1007/978-3-030-10534-1

Caswell, H., de Vries, C., Hartemink, N., Roth, G., & van Daalen, S. F. (2018). Age × stage-classified demographic analysis: a comprehensive approach. *Ecological Monographs*, *88*(4), 560–584. https://doi.org/10.1002/ecm.1306

Chen, Z., Dassios, A., & Tzougas, G. (2023). INAR approximation of bivariate linear birth and death process. *Statistical Inference for Stochastic Processes*, *26*(3), 459–497. https://doi.org/10.1007/s11203-023-09289-9

Czuppon, P., & Traulsen, A. (2021). Understanding evolutionary and ecological dynamics using a continuum limit. *Ecology and Evolution*, *11*(11), 5857–5873. https://doi.org/10.1002/ece3.7205

Di Crescenzo, A., & Paraggio, P. (2019). Logistic Growth Described by Birth-Death and Diffusion Processes. *Mathematics*, *7*(6), 489. https://doi.org/10.3390/math7060489

DiLeonardo, S. L. (2018). *Stochastic Population Dynamics.* Staten Island: City University of New York.

Feng, T., Zhou, H., Qiu, Z., & Kang, Y. (2022). Impacts of demographic and environmental stochasticity on population dynamics with cooperative effects. *Mathematical Biosciences*, *353*, 108910. https://doi.org/10.1016/j.mbs.2022.108910

Ferreira, M. F. (2014). *Stochastic Differential Equation Models in Population Dynamics.* Universidade de Coimbra.

for stochastic differential equations with state-dependent Markovian switching driven by -stable process. *Numerical Algorithms, 101*, 2269 - 2299. doi:10.1007/s11075-025-02087-9

Gardner, C. W. (2009). *Stochastic Methods: A Handbook for the Natural and Social Sciences.* Berlin, Heidelberg: Springer.

Gompertz, B. (1825). On the nature of the function expressive of the law of human mortality and on a new model of determining life contingencies. *Philosophical Transactions of the Royal Society*, *115*, 513–585. doi:10.1098/rspl.1815.0271

Grilli, J. (2020). Macroecological laws describe variation and diversity in microbial communities. *Nature Communications*, *11*(1). https://doi.org/10.1038/s41467-020-18529-y

Guo, Q. (2014). Central-marginal population dynamics in species invasions. *Frontiers in Ecology and Evolution*, *2*. https://doi.org/10.3389/fevo.2014.00023

He, Z., Hui, Z., Sheng, C., Su, B., & Tao, Z. (2026). Quasi-monte carlo based meshfree methods for parabolic equations on parameterized riemannian manifolds (2610.23341V1). arXiv.

© 2026 The Authors. Published by Bexford Publishing Ltd

https://arxiv.org/abs/2610.23341v1

Hernandez-Suarez, C. (2023). Back to the future: A simplified and intuitive derivation of the Lotka-Euler equation. *arXiv*.

Heydari, J., Lawless, C., Lydall, D. A., & Wilkinson, D. J. (2014). Fast Bayesian parameter estimation for stochastic logistic growth models. *Biosystems*, *122*, 55–72. https://doi.org/10.1016/j.biosystems.2014.05.002

Higham., D. J. (2001). An Algorithmic Introduction to Numerical Simulation of Stochastic Differential Equations. *SIAM Review*, *43*(3), 525–546. https://doi.org/10.1137/s0036144500378302

Hu, H., Xu, L., & Wang, K. (2018). A comparison of deterministic and stochastic predator-prey models with disease in the predator. *Discrete and Continuous Dynamical Systems - B*, *24*(6), 2837–2863. https://doi.org/10.3934/dcdsb.2018289

Huang, X. (2011). Quasi‐maximum likelihood estimation of discretely observed diffusions. *The Econometrics Journal*, *14*(2), 241–256. https://doi.org/10.1111/j.1368-423x.2010.00324.x

Huo, L., & Cho, J. S. (2020). Testing for the sandwich-form covariance matrix of the quasi-maximum likelihood estimator. *TEST*, *30*(2), 293–317. https://doi.org/10.1007/s11749-020-00719-x

Ignatieva, A., Hein, J., & Jenkins, P. A. (2020). A characterisation of the reconstructed birth–death process through time rescaling. *Theoretical Population Biology*, *134*, 61–76. https://doi.org/10.1016/j.tpb.2020.05.001

Ikegwu, E. M., & Nkemnole, E. B. (2025). Migration Modified Stochastic Logistic Growth Model: Development, Characterisation Solutions and Applications to Nigeria Population. *Journal of Science Innovation and Technology Research*, *7*(9). https://doi.org/10.70382/ajsitr.v7i9.033

Infante, S., Sanchez, L., & Hernandez, A. (2019). Stochastic Models to Estimate Population Dynamics. *Statistics, Optimisation and Information Computing, 7*, 311-328.

Ivanenko, D. O., & Pogorielov, R. V. (2023). QML parameter estimation in diffusion models. *AIP Conference Proceedings*, *2797*, 050026–050026. https://doi.org/10.1063/5.0160877

Jalal, H., & Alarid-Escudero, F. (2017). A gaussian approximation approach for value of information analysis. *Medical Decision Making*, *38*(2), 174–188. https://doi.org/10.1177/0272989x17715627

Kawano, T., Wallbridge, N., & Plummer, C. (2020). Logistic Models for Simulating the Growth of Plants by Defining the Maximum Plant Size as the Limit of Information Flow. *Plant Signaling & Behavior*, 1709718. https://doi.org/10.1080/15592324.2019.1709718

Kloeden, P. E., & Platen, E. (1992). Numerical Solution of Stochastic Differential Equations. In *Springer eBooks*. Springer Nature. https://doi.org/10.1007/978-3-662-12616-5

Kozlov, V., Radosavljevic, S., Tkachev, V. G., & Uno Wennergren. (2021). Global stability of an age-structured population model on several temporally variable patches. *Journal of Mathematical Biology*, *83*(6-7). https://doi.org/10.1007/s00285-021-01701-3

Malthus, T. R., (1898). An Essay on the Principle of Population, as it Affects the future improvement of Society: With remarks on the speculations of Mr Godwin M. Condorcet and other writers. 7th edition. Harmondsworth: Penguin

Marinoschi, G. (2017). Rescaling approach for a stochastic population dynamics equation perturbed by a linear multiplicative Gaussian noise. *arXiv preprint*, arXiv:1710.02655v1.

© 2026 The Authors. Published by Bexford Publishing Ltd

Marrec, L., Bank, C., & Bertrand, T. (2023). Solving the stochastic dynamics of population growth. *Ecology and Evolution, 13*(8), e10295. doi:10.1002/ece3.10295

Matis, J. H., & Kiffe, T. R. (2004). On Stochastic Logistic Growth Models with Immigration and Multiple Births. *Theoretical Population Biology, 65*(1), 89 - 104. doi:10.1016/j.tpb.2003.08.003

McKane, A. J., & Newman, T. J. (2004). Stochastic models in population biology and their deterministic analogs. *Physical Review E*, *70*(4). https://doi.org/10.1103/physreve.70.041902

Mubayi, A., Kribs, C., Arunachalam, V., & Castillo-Chavez, C. (2019). Studying Complexity and Risk Through Stochastic Population Dynamics: Persistence, Resonance, and Extinction in Ecosystems. *Handbook of Statistics*. https://doi.org/10.1016/bs.host.2018.11.001

Méndez, V., Assaf, M., Campos, D., & Horsthemke, W. (2015). Stochastic dynamics and logistic population growth. *Physical Review E*, *91*(6). https://doi.org/10.1103/physreve.91.062133

Naaz, E., & Ahmad, N. (2025). Numerical Accuracy of Euler-Maruyama and Milstein Methods for Solving Nonlinear Stochastic Differential Equations. *Communications on Applied Nonlinear Analysis, 32*(10), 3223-3237.

Ogethakpo, A. J., & Ojobor, S. A. (2021). The Lotka-Volterra Predator-Prey Model with Disturbances. *Nigerian Journal of Science and Environment, 19*(2), 135 - 144.

Padilla, P. P. (2012). The WKB Approximation. *Undergraduate Lecture Notes in Physics*, 129–154. https://doi.org/10.1007/978-3-642-29378-8_6

Pearl, R., & Reed, L. J. (1920). On the rate of growth of the population of the United States since 1790 and its mathematical representation. *Proceedings of the National Academy of Sciences of the United States of America. 6*, pp. 275 - 288. National Academy of Sciences.

Pelagalli, C., Faccio, S., & Casari, P. (2025). Mathematical Modeling and Simulation of Logistic Growth. *Applied Sciences*, *15*(8), 4409–4409. https://doi.org/10.3390/app15084409

Prettner, K., & Bloom, D. E. (2020). Rethinking Economic Growth in a Post-Pandemic World. *Finance & Development*, *57*(4), 6–10.

Rihan, F. A., & Alsakaji, H. J. (2020). Stochastic delay differential equations of three-species prey-predator system with cooperation among prey species. *Discrete & Continuous Dynamical Systems - S*, *0*(0), 0. https://doi.org/10.3934/dcdss.2020468

Shoemaker, W. R., Álvaro Sánchez, & Grilli, J. (2025). Macroecological patterns in experimental microbial communities. *PLoS Computational Biology*, *21*(5), e1013044–e1013044. https://doi.org/10.1371/journal.pcbi.1013044

Sigmund, K. (2007). Kolmogorov and population dynamics. *Springer EBooks*, 177–186. https://doi.org/10.1007/978-3-540-36351-4_9

Simpson, M. J., Baker, R. E., Buenzli, P. R., Nicholson, R., & Maclaren, O. J. (2022). Reliable and efficient parameter estimation using approximate continuum limit descriptions of stochastic models. *Journal of Theoretical Biology*, *549*, 111201–111201. https://doi.org/10.1016/j.jtbi.2022.111201

Sojecka, A. A., & Drozd-Rzoska, A. (2024). Global population: from Super-Malthus behavior to Doomsday criticality. *Scientific Reports*, *14*(1). https://doi.org/10.1038/s41598-024-60589-3

Stutz, A. J. (2014). Modeling the Pre-Industrial Roots of Modern Super-Exponential Population Growth.

© 2026 The Authors. Published by Bexford Publishing Ltd

PLoS ONE, *9*(8), e105291. https://doi.org/10.1371/journal.pone.0105291

Taagepera, R., & Nemčok, M. (2023). World population growth over millennia: Ancient and present phases with a temporary halt in-between. *The Anthropocene Review*, *11*(1), 205301962311724-205301962311724. https://doi.org/10.1177/20530196231172423

Tarasov, V. E. (2021). Predator‐prey models with memory and kicks: Exact solution and discrete maps with memory. *Mathematical Methods in the Applied Sciences*, *44*(14), 11514–11525. https://doi.org/10.1002/mma.7510

Tesfay, A., Saeed, T., Zeb, A., Tesfay, D., Khalaf, A., & Brannan, J. (2021). Dynamics of a stochastic COVID-19 epidemic model with jump-diffusion. *Advances in Difference Equations*, *2021*(1). https://doi.org/10.1186/s13662-021-03396-8

Uchida, M. (2009). Contrast-based information criterion for ergodic diffusion processes from discrete observations. *Annals of the Institute of Statistical Mathematics*, *62*(1), 161–187. https://doi.org/10.1007/s10463-009-0245-1

Uchida, M., & Yoshida, N. (2013). Quasi likelihood analysis of volatility and nondegeneracy of statistical random field. *Stochastic Processes and Their Applications*, *123*(7), 2851–2876. https://doi.org/10.1016/j.spa.2013.04.008

UN DESA. (2024). *World Population Prospects 2024*. United Nations; United Nations Department of Economic and Social Affairs. https://population.un.org/wpp/

Usman, A. S. (2025). Enhanced Population Projection for Taraba State, Nigeria Using Runge-Kutta-Fehlberg Method in Improved Logistics Modeling. *Journal of Science Innovation & Technology Research (JSITR)*, *7*(9), 12/137. https://doi.org/10.70382/ajsitr.v7i9.014

Verhulst, P. F. (1838). Mathematical research on the law of population growth. *New Memories of the Royal Academy of Sciences and Beautiful Letters of Brussels, 18*, 1–41.

Veron, P., Andréoletti, J., Giraud, T., & Morlon, H. (2025). Speciation completion rates have limited impact on macroevolutionary diversification. *Philosophical Transactions of the Royal Society B: Biological Sciences*, *380*(1919). https://doi.org/10.1098/rstb.2023.0317

Wang, S., & Niu, L. (2025). On the Global stability of a discrete-time predator-prey model of Kolmogorov type. *Discrete and Continuous Dynamical Systems - B*, *30*(9), 3526–3540. https://doi.org/10.3934/dcdsb.2025033

Wang, L., & Zhou, Q. (2026). Strong and weak convergence rates of Euler-Maruyama scheme

World Bank. (2025). *World Development Indicators*. The World Bank. https://databank.worldbank.org/source/world-development-indicators

Yoshida, N. (2025). Quasi-likelihood analysis for nonlinear stochastic processes. *Econometrics and Statistics*, *33*(C), 246–257. https://doi.org/10.1016/j.ecosta.2022.04.002

Yu, X., & Ma, Y. (2023). Noise-induced dynamics in a single species model with Allee effect driven by correlated colored noises. *Journal of Theoretical Biology*, *573*, 111610. https://doi.org/10.1016/j.jtbi.2023.111610

Zhao, Q., & Niu, X. (2024). Dynamics of a Stochastic Predator–Prey Model with Smith Growth Rate and Cooperative Defense. *Mathematics*, *12*(12), 1796–1796. https://doi.org/10.3390/math12121796

Zinihi, A., Sidi, R., & Ehrhardt, M. (2025). Dynamical behavior of a stochastic epidemiological model:

© 2026 The Authors. Published by Bexford Publishing Ltd

stationary distribution and extinction of a SIRS model with stochastic perturbations. *SeMA Journal*. https://doi.org/10.1007/s40324-025-00381-z



© 2026 by the authors. Submitted for possible open access publication under the terms and conditions of the **Creative Commons Attribution (CC BY 4.0) licence** (https://creativecommons.org/licenses/by/4.0/)